UNIVERSITY OF TURKU

IMPROVING THE EFFICIENCIES OF PHOTOAUTOTROPHIC BIOFUEL PRODUCTION: FROM BIOMASS TO BIOCATALYSTS

Mikael Jämsä

TURUN YLIOPISTON JULKAISUJA – ANNALES UNIVERSITATIS TURKUENSIS
SARJA - SER. AI OSA - TOM. 608 | ASTRONOMICA - CHEMICA - PHYSICA – MATHEMATICA | TURKU 2019

UNIVERSITY OF TURKU

IMPROVING THE EFFICIENCIES OF PHOTOAUTOTROPHIC BIOFUEL PRODUCTION: FROM BIOMASS TO BIOCATALYSTS

Mikael Jämsä

TURUN YLIOPISTON JULKAISUJA – ANNALES UNIVERSITATIS TURKUENSIS
SARJA - SER. AI OSA - TOM. 608 | ASTRONOMICA - CHEMICA - PHYSICA – MATHEMATICA | TURKU 2019

University of Turku

Faculty of Science and Engineering
Department of Biochemistry
Laboratory of Molecular Plant Biology
Doctoral Programme in Molecular Life Sciences

Supervised by

Assoc. Prof. Yagut Allahverdiyeva-Rinne
Laboratory of Molecular Plant Biology
Department of Biochemistry
University of Turku
Turku, Finland

Dr. Fiona Lynch
Laboratory of Molecular Plant Biology
Department of Biochemistry
University of Turku
Turku, Finland

Academician Eva-Mari Aro
Laboratory of Molecular Plant Biology
Department of Biochemistry
University of Turku
Turku, Finland

Reviewed by

Prof. Amit Bhatnagar
Water Chemistry and Microbiology Research Group
Department of Environmental and Biological Sciences
University of Eastern Finland
Finland

Assoc. Prof. Raffaella Villa
School of Engineering and Sustainable Development
Faculty of Computing, Engineering and Media
De Montfort University
United Kingdom

Opponent

Assoc. Prof. Raúl Muñoz Torre
Department Chemical Engineering and Environmental Technology
University of Valladolid
Spain

The originality of this thesis has been checked in accordance with the University of Turku quality assurance system using the Turnitin Originality Check service.

ISBN 978-951-29-7683-6 (PRINT)
ISBN 978-951-29-7684-3 (PDF)
ISSN 0082-7002 (Print)
ISSN 2343-3175 (Online)
Grano Oy - Turku, Finland 2019

TURUN YLIOPISTO
Luonnontieteiden ja tekniikan tiedekunta
Biokemian laitos
Molekulaarinen kasvibiologia
MIKAEL JÄMSÄ: Improving the efficiencies of photoautotrophic biofuel production: from biomass to biocatalysts
Väitöskirja, 130 s.
Molekulaaristen biotieteiden tohtoriohjelma
Toukokuu 2019

Tiivistelmä

Yhä kasvavat ilmastonmuutoksen, resurssiniukkuuden ja ympäristön saastumisen aiheuttamat haitat vaativat uutta kestävämpää tapaa energian ja kemikaalien tuotantoon. Yhteyttävät mikrobit, jotka sisältävät syanobakteerit ja viherlevät, ovat lupaavia lähtöaineita niiden tuotantoon, koska niiden tuotto pinta-alaa kohden on suuri, eikä niiden kasvatus kilpaile ruuantuotannon kanssa. Lisäksi ne soveltuvat haluttujen polttoaineiden ja kemikaalien tuotantoon eräänlaisina biokatalyytteinä, jolloin solu tuottaisi näitä lopputuotteita ilman erillistä jalostusvaihetta. Kuitenkin tarvitaan vielä merkittäviä parannuksia tuottotehokkuuteen, jotta näiden biokatalyyttien teollinen käyttö tulisi kannattavaksi.

Väitöskirjan aiheena on tehostaa yhteyttävien mikrobien tehokkuutta eri sovelluksissa. Tämän tavoitteen saavuttamiseksi työssä tutkittiin kahta eri lähestymistapaa: (i) yhdistetty biomassapohjainen tuotanto ja (ii) suora biopolttoaine-/kemikaalituotanto. Ensimmäisessä lähestymistavassa sovellettiin yhdistettyä jätevedenpuhdistusta ja biopolttoaineiden tuotantoa hyödyntäen suomalaisia mikroleväkantoja. Leväkantojen seulonnassa UHCC0027 levälaji osoittautui lupaavaksi ravinteiden kerääjäksi. Lisäksi se oli tehokas rasvapitoisuuden keräämisessä. Pilotti-mittakaavassa se osoitti tehokasta ravinteiden sitomista oikeassa jätevedessä useissa eri olosuhteissa (mm. korkea ja matala orgaanisen aineen pitoisuus ja eri lämpötilat). Ravinteiden suhteilla (C:N ja N:P) oli tärkeä rooli biomassan kasvussa ja ravinteiden sitomisnopeudessa. Rasvahappojen metyyliesterien profiilit eivät täyttäneet sekoittamattoman biodieselin vaatimuksia, mikä voidaan välttää esimerkiksi hydrogenoimalla rasvahapot.

Toinen lähestymistapa oli syanobakteerien ja viherleväsolujen immobilisointi TEMPO-hapetettuihin selluloosa nanofibrilleihin (TEMPO CNF), mikä tehtiin ensimmäistä kertaa tämän väitöskirjatyön puitteissa. Immobilisointi mahdollistaa

useimmiten käytettyjen liuosmaisten kasvatusten siirtämisen kiinteään matriisiin. Tämä puolestaan tehostaa solujen energiatehokkuutta lopputuotteiden suuntaan, kun solujen jakaantuminen saadaan pysäytettyä. Lisäksi immobilisointi säilyttää fotosynteettisten solujen biokatalyyttisen aktiivisuuden pidempään. Tässä lähestymistavassa käytettiin kolmea eri metodia: (i) puhdas TEMPO CNF hydrogeeli; (ii) $Ca2^{+}$-ioneilla stabilisoitu TEMPO CNF hydrogeeli; ja (iii) polyvinyylialkoholilla (PVA) ristisilloitettu kiinteä TEMPO CNF filmi. Tärkeimpiä tuloksia olivat TEMPO CNF immobilisoitujen *Chlamydomonas reinhardtii* viherlevien korkeampi vedyntuotto (verrattuna alginaatti verrokkiin) ja *Anabaena* sp. PCC7120 Δ*hupL* solujen tehokas vedyntuotto kuivausvaiheen jälkeen. Kuivausvaihe tarvittiin jäykän ja vahvan filmin aikaansaamiseksi.

Yhteenvetona voidaan todeta, että tämä väitöskirjatyö osoitti lupaavia tapoja mikrolevillä tehtävän jätevedenpuhdistuksen ja biopolttoaineiden tuotannon tehostamiseksi. Lisäksi ensikertaa mikroleväsolujen immobilisointiin käytetyllä TEMPO CNF nanoselluloosalla on monia ominaisuuksia, kuten huokoisuus ja mekaaninen vahvuus, jotka parantavat biokatalyyttien tuottotehokkuutta.

Avainsanat: mikrolevä, jätevedenpuhdistus, biodiesel, nanoselluloosa, vety

UNIVERSITY OF TURKU
Faculty of Science and Engineering
Department of Biochemistry
Molecular Plant Biology
MIKAEL JÄMSÄ: Improving the efficiencies of photoautotrophic biofuel production: from biomass to biocatalysts
Doctoral Dissertation, 130 pp.
Doctoral Programme in Molecular Life Sciences
May 2019

Abstract

The rising effects of climate change and global problems of resource scarcity and environmental pollution require a change in paradigm towards sustainable energy and chemicals production. Photosynthetic microbes, including cyanobacteria and green algae, are promising raw materials for future production platforms which have high aerial productivity and don't compete with food and feed. They are also well suited to act as chassis for the direct and continuous production of targeted fuels and chemicals, thus functioning as true biocatalysts. However, efficiencies of photoautotrophic production system need improvement before a successful shift to these platforms.

The overall aim of this thesis is to improve efficiencies of photoautotrophic production platforms. To meet this aim, I have studied two approaches: (i) Integrative biomass-based production; and (ii) Direct biofuel/chemical production. The first approach involved the integration of wastewater treatment with biofuel production, using native Finnish microalgae. Screening revealed the native alga UHCC0027 as a suitable candidate for efficient nutrient removal and lipid accumulation. At pilot scale, UHCC0027 demonstrated robust nutrient removal performance in real wastewater of both high and low organic loading and at different temperatures, including a cold temperature relevant to Nordic conditions. Nutrient balances (C:N and N:P) were important in biomass accumulation and nutrient removal performance. Whilst Fatty acid methyl ester (FAME) profiles did not meet requirements of unblended fuel standards, workarounds such as hydrogenation may succeed in future.

The second approach involved the immobilization of cyanobacterial and green algal cells in a novel tunable immobilization material, TEMPO oxidized cellulose nanofibrils (TEMPO CNF). This transfers the capabilities of current suspension

photosynthetic cell factories to a solid-state that restricts loss of energy to biomass accumulation and enables photosynthetic cells to operate as long-living true catalysts for bioproduction. Three different construction methods were used: (i) a pure TEMPO CNF hydrogel; (ii) a Ca^{2+}-stabilized TEMPO CNF hydrogel; and (iii) a polyvinyl alcohol (PVA) crosslinked solid TEMPO CNF film. Important outcomes were the considerably higher hydrogen yields of TEMPO CNF immobilized *Chlamydomonas reinhardtii* (compared to alginate controls) and the recovery and efficient hydrogen production of *Anabaena* sp. PCC7120 Δ*hupL* cells after drying. Drying was required for stable film formation and presents an opportunity for scaffold-free films in future.

Overall, this thesis presents work demonstrating promising optimizations for improving efficiencies of microalgal wastewater treatment and biofuel (chemicals) production. Additionally, the novel employment of TEMPO CNF immobilization matrix for photobiological hydrogen production is an important step to addressing porosity and mechanical stability limitations of current immobilization techniques.

Keywords: microalgae, wastewater treatment, biodiesel, nanocellulose, hydrogen

Table of Contents

List of original publications

This thesis is composed of the following scientific articles, referred to in the text by their Roman numerals.

I. Lynch, F., Santana-Sánchez, A., Jämsä, M., Sivonen, K., Aro, E.-M., Allahverdiyeva, Y. (2015) Screening native isolates of cyanobacteria and a green alga for integrated wastewater treatment, biomass accumulation and neutral lipid production. *Algal Res.* 11, 411-420. doi:10.1016/j.algal.2015.05.015

II. Jämsä, M.*, Lynch, F.*, Santana-Sánchez, A., Laaksonen, P., Zaitsev, G., Solovchenko, A., Allahverdiyeva, Y. (2017) Nutrient removal and biodiesel feedstock potential of green alga UHCC00027 grown in municipal wastewater under Nordic conditions. *Algal Res.* 26, 65-73. doi: 10.1016/j.algal.2017.06.019 *Shared first authorship

III. Jämsä, M.*, Kosourov, S.*, Rissanen, V.*, Hakalahti, M., Pere, J., Ketoja, J.A., Tammelin, T., Allahverdiyeva, Y. (2018) Versatile templates from cellulose nanofibrils for photosynthetic microbial biofuel production. *J. Mater. Chem. A* 6, 5825-5835. doi:10.1039/C7TA11164A *Shared first authorship

Abbreviations

[FeFe]	Iron–iron cluster, which the active site of [FeFe]-hydrogenase
[Ni–Fe]	Nickel–iron cluster, which the active site of [Ni–Fe] hydrogenase
ADP	Adenosine-5'-diphosphate
APHA	American Public Health Association
ATP	Adenosine-5'-triphosphate
BG11	growth medium for cyanobacteria
BODIPY	4,4-difluoro-4-bora-3a,4a-diaza-s-indacene
C16:0	Acyl-chain with 16 carbon atoms
C16:1	Acyl-chain with 16 carbon atoms with one double bond
C16:4	Acyl-chain with 16 carbon atoms with four double bonds
C18:1	Acyl-chain with 18 carbon atoms with one double bond
C18:3	Acyl-chain with 18 carbon atoms with three double bonds
C18:4 FA	18 carbon long fatty acid with four double bonds
C18:4me	18 carbon long fatty acid methyl ester with four double bonds
C20:5	20 carbon long fatty acid methyl ester with five double bonds
CCM	Carbon dioxide concentrating mechanism
CFL	Compact fluorescent lamp
CNF	Cellulose nanofibrils
CO_2	Carbon dioxide
COD	Chemical oxygen demand
Cyt c6	Cytochrome c6 electron-transfer protein
Cytbf	Same as Cytochrome b_6f complex
DNA	Deoxyribonucleic acid
EPA	Eicosapentaenoic acid
EPS	Extracellular polymeric substances
FAAE	Fatty acid alkyl ester
FAME	Fatty acid methyl ester
Fm′	Maximum fluorescence level in light
FNR	Ferredoxin−NADP+ reductase enzyme
Ft	Steady-state chlorophyll a fluorescence level

HC_LN	Experiment performed with wastewater having high COD concentration and lower nutrient concentrations
HEPES	4-(2-hydroxyethyl)-1-piperazineethanesulfonic acid
HRAP	High rate algal pond
ICN	International Code of Nomenclature for Algae, Fungi and Plants
ICNP	International Code for Nomenclature of Prokaryotes
LC_HN	Experiment performed with wastewater having lower COD concentration and higher nutrient concentrations
LC_HN cold	Experiment performed with wastewater having lower COD concentration and higher nutrient concentrations under Finnish spring and autumn temperatures
Mn	Manganese
mt−	Mating type locus −
$NADP^+$	Nicotinamide adenine dinucleotide phosphate (oxidized)
NADPH	Nicotinamide adenine dinucleotide phosphate (reduced)
NH_4^+-N	Ammoniacal nitrogen
NiR	Nitrite reductase enzyme
nit−	Mutations at the *nit1* and *nit 2* genes, making the strain unable to grow on nitrate as nitrogen source
NM	Not measured
NO_2^--N	Nitrite nitrogen
NO_3^--N	Nitrate nitrogen
NR	Nitrate reductase enzyme
OD	Optical density
OD_{750nm}	Optical density measured at 750 nm wavelength
P680	Primary electron donor of Photosystem II
P680*	Excited primary electron donor of Photosystem II
$P680^+$	Oxidized primary electron donor of Photosystem II
P700	Primary electron donor of Photosystem II
PAR	Photosynthetically active radiation (400 nm to 700 nm wavelengths)
PBR	Photobioreactor
PBS	Phosphate-buffered saline
Pc	Plastocyanin protein
PEI	Polyethylenimine
pH	Negative logarithm of the proton concentration
pmf	Proton motive force
PO_4^{3-}-P	Orthophosphate phosphorus
ppm	Parts per million

PQ	Plastoquinone
PSI	Photosystem I
PSII	Photosystem II
PVA	Poly(vinyl alcohol)
QA	Primary electron acceptor of Photosystem II
QB	Secondary electron acceptor of Photosystem II
QCM-D	Quartz crystal microbalance with dissipation monitoring
RuBisCO	Ribulose bisphosphate carboxylase/oxygenase
SD	Standard deviation
sp.	Species
TAP	Tris-Acetate-Phosphate growth medium for green algae
TAP-S-P	TAP-minus-sulfur-minus phosphorus medium
TEMPO	2,2,6,6-Tetramethylpiperidin-1-oxyl
TEMPO CNF	2,2,6,6-Tetramethylpiperidin-1-oxyl oxidized cellulose nanofibrils
UHCC	University of Helsinki Culture Collection
UWWTD	European Union Urban Waste Water Treatment Directive 91/271/EEC
wt%	Weight percentage
Y(II)	Effective photosystem II yield
Z8x	Z8 growth medium for cyanobacteria without combined nitrogen
Δ*hupL*	Deletion mutant of uptake hydrogenase large subunit gene

1 INTRODUCTION

1.1 Climate change

The discovery of oil and other fossil fuels was one of the crucial factors that evolved the second industrial revolution in the mid-19th century. Ever since, oil has been involved in most people's everyday lives in developed countries (Stearns, 2012). Exploitation of fossil energy will always yield carbon dioxide (CO_2) emission into the atmosphere. However, it was only realized late in the 20th century that the most likely reason behind increased average global temperatures was CO_2 emissions (Fleming, 2005). The CO_2 concentration in the atmosphere has increased 70 ppm within just forty years (Figure 1.) and in 2016, 400 ppm was exceeded. In line with the rising CO_2 level, the global average temperature has increased half a degree (Hansen et al., 2010).

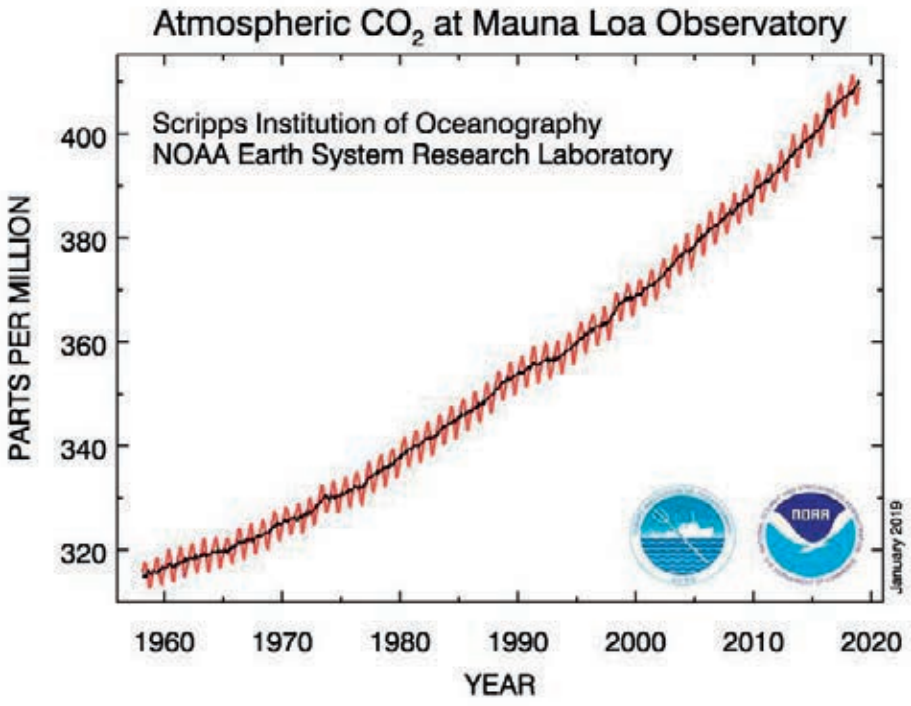

Figure 1. Monthly CO_2 concentrations in the Earth´s atmosphere over the last fifty years, measured at Mauna Loa Observatory, Hawaii. Data source: National Oceanic and Atmospheric Administration, https://www.noaa.gov/ (accessed: 4.2.2019)

Since the beginning of the 20th century, it has been predicted that oil production would peak in the near future (White, 1919). The situation was changed when the exploitation of shale oil became feasible. Since then, the discourse has turned to how much of the existing fossil resources can be used without disturbing the climate too much. When the Paris agreement was negotiated in 2015, it was pursued to limit the global average temperature increase to 1.5 degrees Celsius. That would mean significant amounts of fossil energy would need to remain in the Earth´s crust. For instance, it has been proposed that one third of the oil, half of the gas and 80% of the coal reservoirs of the Earth should remain unexploited in order to limit the temperature increase to two degrees (McGlade and Ekins, 2015).

It has been estimated that 28% of the emissions resulting from fossil energy exploitation is absorbed by terrestrial biota. The contribution of oceans is 27% and the remaining 46% stays in the atmosphere (Le Quéré et al., 2012). Natural CO_2

absorption, followed by conversion to biomass, is almost solely driven by photosynthetic organisms (Lal, 2008). Photosynthetic organisms can thus be employed in a biotic approach to sequester carbon toward balancing the net flux between fossil carbon and atmospheric carbon. Both biotic and abiotic approaches, such as concentrated CO_2 injection into the depths of oceans and deep geological strata and CO_2 mineralization, have been considered. Biotic carbon sequestration strategies rely on photosynthetic organisms in aquatic and terrestrial environments, including *e.g.* afforestation and iron fertilization of oceans to boost phytoplankton growth. Besides the aforementioned strategies, a shift away from fossil fuels and products toward the production of biofuels and bioproducts will help balance the carbon fluxes (Lal, 2008) and play an important role in shifting social perceptions and economic structures toward required change.

1.2 Photosynthesis and its contribution to CO_2 mitigation

In photosynthesis, the energy of visible light is converted to chemical energy. This mechanism involves multiple proteins, pigment molecules and redox components in order to work seamlessly.

$6\ CO_2 + 6\ H_2O \rightarrow C_6H_{12}O_6 + 6\ O_2$ (**Equation 1**, general equation of photosynthesis)

The main pigment-protein complexes driving this process are photosystem I and II (PSI & PSII) which are attached to the thylakoid membrane (Figure 2). Photosynthesis begins when the pigment molecules in the photosynthetic light-harvesting antenna absorb light energy. This energy travels by Förster resonance energy transfer between chlorophyll molecules to P680, or P700. P680 and P700 are special chlorophyll dimers, located at the reaction centers of the photosystems and are the primary donors of PSII and PSI, respectively. Charge separation in PSII occurs between excited P680* and a pheophytin molecule. From pheophytin, electrons are transferred to PSII bound QA and QB plastoquinone molecules. Double protonated plastoquinol molecules leave the QB binding pocket to the plastoquinone pool and donate electrons to the cytochrome b_6f complex. This complex mediates electron transfer between PSII and PSI. The cytochrome b_6f complex transfers electrons to the small plastocyanin (or Cyt c6) protein that reduces the oxidized P700 chlorophyll dimer (Romero et al., 2017).

Oxidized P680 ($P680^+$) recovers the missing electron from water splitting at the Mn-cluster, which is located on the donor side of PSII. The Mn-cluster, consisting of five oxygen, four manganese and one calcium atom, is located on the lumenal side of the

thylakoid membrane, as part of the PSII complex (Dekker and Boekema, 2005; Umena et al., 2011).

Charge separation occurs in the PSI complex in a similar manner to the PSII complex. The oxidized P700 chlorophyll has the highest reductive potential found in nature (Janssen et al., 2012; Van Eerden et al., 2017). From PSI, the excited electrons are transferred via several co-factors to ferredoxin proteins, located on the stromal side of the thylakoid membrane. Finally, nicotinamide adenine dinucleotide phosphate ($NADP^+$) is reduced to NADPH, mediated by the Ferredoxin–$NADP^+$ reductase (FNR) enzyme. The proton-motive force (pmf) created by photosynthetic light reactions is used for adenosine diphosphate (ADP) phosphorylation to Adenosine triphosphate (ATP) (Golbeck, 2006). This process is called linear photosynthetic electron transport.

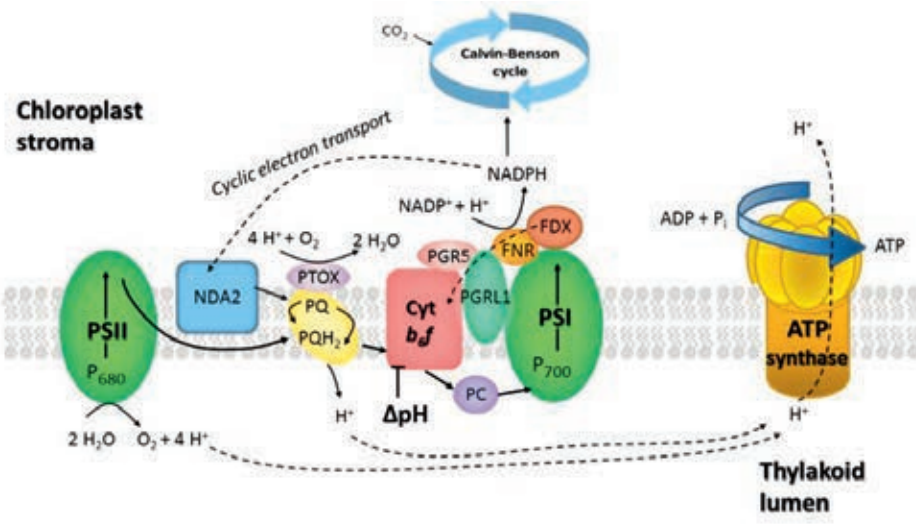

Figure 2. The general scheme of the photosynthesis process around the thylakoid membrane in a eukaryotic cell. Figure kindly provided by Martina Jokel-Toivanen.

Both NADPH and ATP are transported to the stromal side of thylakoid membrane to be used in CO_2 fixation and in other cellular metabolism. Under different environmental stress conditions, *e.g.* fluctuations in light or temperature, or nutrient deprivation, the NADPH/ATP ratio changes in the cell metabolism and alternative electron transport routes start to play a role. These transport mechanisms include many terminal oxidases, which reduce oxygen back to water and the cyclic electron transport that circulates electrons around the PSI complex (Yamori and Shikanai, 2016).

Cyanobacteria and algae have evolved a special compartment for concentrating CO_2 in the near vicinity of the Ribulose-1,5-bisphosphate carboxylase-oxygenase (RuBisCO) enzyme. These compartments are called carboxysomes and pyrenoids in cyanobacteria and algae, respectively (Tomar et al., 2017). In these compartments, bicarbonate that the cells have concentrated is converted to CO_2 by carbonic anhydrase, which is then utilized by RuBisCO. This enzyme is the main enzyme in the twelve-step CO_2 fixation cycle, known as Calvin-Benson-Bassham Cycle. This cycle consumes the NADPH and ATP produced by photosynthetic light reactions. Stoichiometrically, it takes two NADPH and three ATP molecules to fix one CO_2 molecule to become part of carbohydrate molecules (Ebenhöh and Spelberg, 2017).

Photosynthetic organisms fix approximately 15% of all atmospheric carbon annually, which corresponds to 17 times the annually emitted carbon originated from fossil sources. However, most fixed carbon is released back through soil and plant respiration (Lal, 2008) resulting in only 28% being absorbed by terrestrial biota (refer section 1.1). When the absorption of terrestrial and oceanic biotas are summed, only about half of the fossil carbon that is annually emitted into the atmosphere is actually sequestered by oceans and terrestrial biotas (Houghton, 2007). Plants and other terrestrial photosynthetic organisms contribute 54% of the annual CO_2 conversion to biomass, leaving the remaining 46% to aquatic photoautotrophs (Field et al., 1998).

1.3 Photoautotrophic microbes: green algae and cyanobacteria

Green algae and cyanobacteria are photosynthetic organisms which consist a large part of ocean´s biomass (Gasol et al., 1997). From a phylogenetic point of view, they belong to separate biological domains. Cyanobacteria are Gram-negative prokaryotes and green algae are eukaryotes. Cyanobacterial chromosomal DNA is not packed inside a nucleus like in green algae (Stanier and Van Niel, 1962). Cyanobacteria are thought to have created the current high O_2 concentration in the

Earth´s atmosphere during the Great Oxygenation Event about 2.5 billion years ago (Bekker et al., 2004). In that way, they are considered to have enabled heterotrophic life on Earth. Their morphology is extremely variable, as there are unicellular, filamentous, branched filamentous and colonial forms of cyanobacteria (Barsanti and Gualtieri, 2014). Some strains are able to fix atmospheric nitrogen by aid of the nitrogenase enzyme (Zehr et al., 2001), to be discussed in section 1.4.1.1.

It is important to mention that, previously under the International Code of Nomenclature for Algae, Fungi and Plants (ICN), cyanobacteria were also classified as algae under the general name "blue-green algae". Only after the mid-20th century, when the International Code for Nomenclature of Prokaryotes (ICNP) was established, cyanobacteria were included in ICNP (Stanier et al., 1978). However, the term microalgae is still commonly used by phycologists and the biotechnology sector as a convenient description, which collectively refers to both prokaryotic cyanobacteria and eukaryotic green algae (Parker et al., 2015). As such, and in line with the published work contributing to this thesis, the term microalgae will be used collectively, with the terms green algae (*i.e.* microscopic green algae in the thesis context) and cyanobacteria used specifically.

Table 1. Comparison of features between cyanobacteria and green algae

	Cyanobacteria	**Green algae**
Biological domain	Prokaryote (bacteria)	Eukaryote
Typical cell size (diameter)	0.5 – 40 µm (Rich and Maier, 2015)	1 µm to over 1 cm (Smith, 2017)
Location of DNA	Cellular cytoplasm	Nucleus, chloroplast, mitochondria
Respiratory system	Photosynthetic membrane (thylakoid)	Mitochondrion and chlororespiration in chloroplasts
Energy storage	Mainly glycogen and polyhydroxyalkanoates, lipid droplets to some extent	Triacylglycerols (inside lipid droplets) and starch
Carbon concentrating organelle	Carboxysome	Pyrenoid
Cell wall	Peptidoglycan, covered with extracellular polymeric substances in some species (Hoiczyk and Hansel, 2000)	Hydroxyproline-rich glycoproteins and cellulosepectins (Domozych et al., 2012)
Thylakoid membrane location	Cellular cytoplasm	Chloroplast
Light harvesting complexes (LHC)	Soluble external antenna: phycobilisomes which consist of phycobiliproteins (phycoerythrins, phycocyanins, and allophycocyanins); LHC with chlorophyll a, b, d, f. The reaction center possess carotenoids and chlorophyll a, d, f	Membrane bound external LHC Carotenoids and chlorophyll a, b and c.
Mobility and Reproduction	Asexually, lacks locomotory organ (Lee, 2008)	Sexually, flagella act as locomotory organ (Lee, 2008)

Another important difference between cyanobacteria and green algae is the location of the thylakoid membranes, where photosynthesis occurs. In cyanobacteria, these are located in the cellular cytoplasm (Komarek, 2006), whereas in green algae they are located inside special organelles, called chloroplasts (Sun et al., 2016). An ancestral photoautotrophic prokaryote related to cyanobacteria is considered a progenitor of chloroplasts in algae and plants. It is not surprising that the structure of the photosynthetic machinery, including the reaction centers of PSI and PSII, cytochrome b_6f, is similar between prokaryotic cyanobacteria and algal chloroplasts (see paragraph 1.2.). However, light harvesting and the auxiliary electron-transport pathways for maintaining optimal photosynthetic performance have undergone remarkable evolution (Mullineaux, 2014). The light harvesting complex of cyanobacteria consists of huge extrinsic pigment–protein complexes called phycobilisomes, whereas green algae and plants have intrinsic major light harvesting antenna (Kirilovsky, 2015). The phycobilisomes are located on the stromal side of thylakoid membrane and their structure consists of multiple rods, which point to the site where photosystem complexes are bound. Unlike the light harvesting antennas of eukaryotes, whose light absorbing molecules are carotenoids and chlorophyll a and b, the phycobilisomes consist of three different groups of phycobiliproteins (phycoerythrins, phycocyanins, and allophycocyanins). They are able to efficiently absorb green and yellow light whereas chlorophylls are not (Kirilovsky, 2015; Thornber, 1975). Being eukaryotes, green algae have mitochondria, which perform cellular respiration like in other non-photosynthetic eukaryotes (Peltier and Thibault, 1985). Besides this, green algae perform cellular respiration in the chloroplasts, called chlororespiration, (Rumeau et al., 2007). In cyanobacteria, both photosynthesis and respiration occur within the same cellular compartment (thylakoid membrane) and share several redox-components (PQ-pool, Cytbf, Pc/Cytc6). Such close interaction between these two main bioenergetic processes strongly affects the regulation of the cellular metabolism (Peschek et al., 2004; Vermaas, 2001). A detailed comparison of the features between cyanobacteria and green algae is presented in the Table 1.

1.4 Microalgal cultivation systems

The most commonly used microalgae cultivation systems are open ponds, particularly high rate algal ponds (HRAPs, figure 3 A). They are usually under half a meter deep and mixing is achieved using a paddle wheel. The size of HRAPs vary from liters of volume (pilot-scale) to hectares of area (full scale) (Craggs et al., 2010). The main benefits of pond cultivation is the inexpensive set-up and maintenance. However, they suffer from many undesirable features, such as

contamination by other phototrophic organisms and grazers. Productivity is rather low and they suit only the species that are possibly to cultivate axenically or by applying selective pressure (Narala et al., 2016). In table 2, a detailed comparison of the differences in microalgal cultivation systems can be found.

Table 2. Comparsion of the differences in microalgal cultivation systems (Sources: Takenaka and Yamaguchi, 2014; Singh and Sharma, 2012; Narala et al., 2016)

	Open pond	closed PBR
Productivity	low	high
Cost of biomass	low	high
Contamination risk	high	low
Energy requirements	low	high
Obtained biomass	varies in quality	uniform
Space required	low	high
Mixing	paddle wheel	pumping or aeration
Cooling	evaporation	water spray and cooling jackets
Risk of overly high oxygen levels	low	high
Suitability for monoculture	poor	good

When higher productivities and higher quality of biomass is needed, closed photobioreactors are generally preferred. The material and set-up costs are significantly higher than HRAPs. There are a wide variety of different PBRs, the fundamental requirement being transparency in some of the construction material, in order to allow the light penetration required for photosynthesis. This feature differentiates them from standard bioreactors. Common examples of PBR configurations are tubular (figure 3B) and flat-panel (figure 3C) reactors. Tubular reactors are composed of horizontally aligned, long transparent tubes connected to each other using ‘u-shaped’ end joints. The tubes are made of plastic or glass and generally have diameters of less than ten centimeters. Flat-panel PBRs are vertically aligned, rectangular boxes with a thin cross section to allow efficient light utilization.

Flat-panel PBRs are mixed by injecting air from the bottom, whereas tubular reactors are mixed via pumping of the liquid phase inside the PBRs (Takenaka and Yamaguchi, 2014).

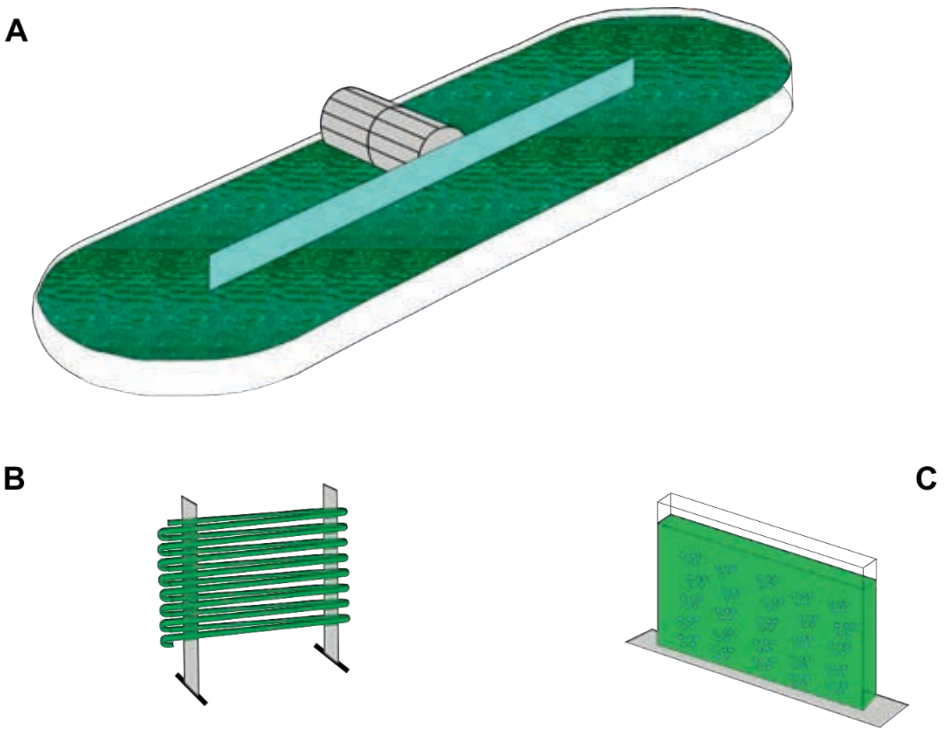

Figure 3. Illustrations of different microalgal cultivation systems: (a) High rate algal pond (HRAP), (b) Tubular photobioreactor and (c) Flat panel photobioreactor

1.5 Biofuels to tackle climate change

The justification for a shift from an oil economy to a bioeconomy is obvious. However, as there is already a history of over one hundred years of oil exploitation, including the research, product development and production of oil based products, the paradigm shift will require a great amount of effort. As mentioned earlier, the realization of climate change has invoked a response in governments and companies to begin the shift towards a cleaner bioeconomy. In fact, there are already markets for many oil replacement products.

Table 3. Classification, sources and features of different generations of biofuels (Sources: Dahiya et al., 2014 and Aro, 2016)

Biofuel generation classification	Sources	Features
1st generation or conventional (bioethanol, biodiesel, biogas)	Oils and polysaccharides from food crops	Need arable land, currently in use
2nd generation (bioethanol, biogas, hydrogenated vegetable oils (HVO))	Non-food crops, lignocellulosic materials and waste sources	No need for arable land but limited sources, their use is expanding
3rd generation or advanced biofuels (biohydrogen together with the aforelisted generations)	1st and 2nd generation technologies applied to microalgae and fuels from genetically engineered microbes and plants	Do not compete with agriculture, superior yields relative to areal footprint, but extensive R&D needed to make feasible

Biofuels can be classified as first, second and third generation fuels. The first generation biofuels (*e.g.* ethanol from sugarcane) are relatively unsustainable and suffer from ethical issues related to their production, as they directly compete with food and feed production (Singh, 2013). Second generation biofuels include fuels *e.g.* from lignocellulosic biomass and various waste sources, like cooking oils and sawdust (Naik et al., 2010). Microalgal biofuels are considered third generation biofuels due to their potential superior areal production yields and their diversity over second generation biofuels. There are variety of biofuel types able to be produced from microalgae, including hydrogen, methane, various alcohols, hydrocarbons and biodiesel (Lee and Lavoie, 2013).

1.5.1 Biodiesel

One form of biofuel obtained from algal and cyanobacterial biomass is biodiesel. It is an appealing energy carrier since it is suitable for current engines and energy delivery infrastructure (Karatzos et al., 2014). Biodiesel can be produced from any biological material containing lipids with long fatty acid chains. In the production process, the long fatty acid chains from the backbone compound, usually a derivative of glycerol, undergo an acid or base catalyzed transesterification. In this process, an alkyl alcohol group (usually methanol) reacts with the acyl groups, yielding fatty acid alkyl esters (FAAEs, in the case of methanol FAMEs) (Hoekman et al., 2012).

The properties of the obtained biodiesel (mixture of FAMEs) will depend on the saturation profile and length of FAMEs (Knothe et al., 2005). The most important properties of biodiesel include the cetane number, viscosity, oxidation stability and cold filter plugging point. The cetane number describes the ignition properties of the fuel in comparison to cetane. The closer the value is to one hundred, the better the fuel ignites when compressed. The higher the degree of acyl chain unsaturation, the lower the cetane number. Oxidation stability is an important parameter when the biodiesel is stored for a long time under a normal atmosphere and it increases concomitantly with the degree of unsaturation. For good performance in cold conditions, the cold filter plugging point is an important parameter describing how easily the fuel system is clogged. Optimal biodiesel should contain mainly C16:1 and C18:1 fatty acids in order to have suitable properties for use in a diesel engine (Pinzi et al., 2009). Microalgal biomass is known to contain these fatty acids in significant amounts, which has made it a potential candidate for biodiesel raw material (Ohse et al., 2014; Pratoomyot et al., 2005).

High lipid content is desirable for an efficient conversion of biomass to biodiesel. Algal biomass has demonstrated highest frequency in the range of 20 to 25% lipids per dry weight (Williams and Laurens, 2010). When algae are exposed to nitrogen-deprived conditions, fixed carbon will be directed to energy storage in the form of triacylglycerols, located inside lipid droplets in the algal cell. This generally results in a significant increase in the lipid proportion of the cell which may exceed over half of the dry weight (Williams and Laurens, 2010). However, it does present a challenge for efficient lipid production as normal cell growth is ceased during the lipid accumulation phase. Recently, however, Ajjawi et al. (2017) reportedly created a microalga strain capable of accumulating 40% lipids during normal growth phase, resulting in efficient lipid accumulation without sacrificing cell growth.

In cyanobacteria, there has been little reported effect of lipid accumulation under nitrogen starvation, depending on the studied species. Cyanobacterial fixed carbon is mainly directed to carbohydrate synthesis and mainly stored as glycogen (Monshupanee and Incharoensakdi, 2014; Peramuna and Summers, 2014; Williams and Laurens, 2010).

1.5.2 Hydrogen

Hydrogen is an ideal energy carrier in many aspects. It has high energy density per mass and the burning of hydrogen in oxygen yields only pure water. When used in fuel cells, the conversion to kinetic energy is twice as efficient as gasoline combustion engines (Seibert and Torzillo, 2018). In addition, hydrogen can be used in multiple industrial processes like ammonia and methanol production and the cracking of hydrocarbons (Ramachandran and Menon, 1998).

There are multiple ways to produce hydrogen, such as the steam reformation of fossil hydrocarbons and the electrolysis of water (Levalley et al., 2014). The most studied sustainable ways to produce hydrogen are photoelectrochemical water splitting, artificial photosynthesis and biological hydrogen production (Idriss et al., 2015). In photoelectrochemical water splitting, sunlight energy is converted to chemical energy, resembling photovoltaic electricity production with solar panels. However, there are still significant challenges related to photoelectrochemical water splitting, like the need for rare earth elements and precious metals, which makes the process economically unfeasible (Joy et al., 2018; Whang and Apaydin, 2018).

1.5.2.1 Biological photohydrogen production by photosynthetic microbes

Hydrogen production by photosynthetic microbes is a highly attractive way to obtain hydrogen, as only light energy, water and nutrients need to be provided to the microbes. However, certain conditions, generally an anoxic environment, are required. This is due to the inherent oxygen sensitivity of the different enzymes linked to hydrogen production in green algae and cyanobacteria (Seibert and Torzillo, 2018).

Green algae possess [FeFe]-hydrogenase, which is able to generate hydrogen according to equation 2. (Allahverdiyeva et al., 2014; Eroglu and Melis, 2016). The [FeFe]-hydrogenase enzyme is involved in all three green algae based pathways for hydrogen production: a light independent fermentative pathway and two light dependent pathways, further divided into the PSII-dependent and PSII-independent pathways.

$$2\ H^+ + 2\ \text{ferredoxin}_{(\text{reduced})} \rightleftharpoons H_2 + 2\ \text{ferredoxin}_{(\text{oxidized})} \qquad \textbf{(Equation 2)}$$

Of these three pathways, the light dependent, PSII-independent pathway has been considered the most promising for large-scale hydrogen production, after the development of the sulphur deprivation protocol (Melis and Happe, 2001). This protocol uses sulphur deprivation to inhibit PSII activity, resulting in the termination of oxygen evolution and the prolonging of hydrogen production, since oxygen is an irreversible inhibitor of [FeFe]-hydrogenase. When PSII activity is blocked, electrons originate either from intracellular carbon sources, or from the surrounding medium (Chochois et al., 2009). Recently, two new protocols have been developed where the PSII-dependent pathway is used for efficient hydrogen production under nutrient replete conditions. This makes possible the production of hydrogen under strict photoautotrophic conditions, without the need for nutrient deprivation (Kosourov et al., 2018 A; Nagy et al., 2018).

In cyanobacteria, three enzymes are involved in hydrogen metabolism: bidirectional [Ni–Fe] hydrogenase, [Ni–Fe] uptake hydrogenase and nitrogenase. All three enzymes are sensitive to O_2. Bidirectional hydrogenase is involved in dark fermentative hydrogen production as well as in the minimal hydrogen yield observed under a transition from dark to light conditions. Besides this, the nitrogenase enzyme produces hydrogen as a side product of the nitrogen fixation process, according to equation 3. Whereas in the absence of nitrogen the enzyme reduces protons to hydrogen (equation 4) (Allahverdiyeva et al., 2014).

$N_2 + 8\ H^+ + 8\ e^- + 16\ ATP \rightarrow 2\ NH_3 + 16\ (ADP + P_i) + 3\ H_2$ (**Equation 3**)

$8\ H^+ + 8\ e^- + 16\ ATP \rightarrow 16\ (ADP + P_i) + 4\ H_2$ (**Equation 4**)

Cyanobacteria apply different strategies for the temporal or spatial separation of nitrogen fixation from photosynthetic oxygen evolution. Temporal separation is achieved by cells performing photosynthesis under light conditions and utilizing the resultant reducing power to fix the molecular nitrogen in dark conditions. In spatial separation, filamentous cyanobacteria employ specialized cells called heterocysts, which are responsible for overall nitrogen fixation. Heterocysts have an oxygen impermeable cell wall, high respiratory activity and negligible oxygen evolving PSII activity, therefore effectively anoxic conditions can be provided within a single cell. As these heterocyst cells lack detectable PSII activity, the neighboring vegetative cells provide the energy needed for the nitrogen fixation and hydrogen production in the form of carbohydrates (Khanna and Lindblad, 2015; Sakurai et al., 2015). The uptake hydrogenase enzyme is present in almost all of the nitrogen fixing cyanobacteria and its role is thought to be related to the creation of an oxygen free environment for nitrogenase and for the recycling of electrons back to cellular metabolism (Tamagnini et al., 2007).

Out of these aforementioned processes, green algal and cyanobacterial hydrogenase-dependent hydrogen production is regarded to be theoretically more efficient than cyanobacterial nitrogenase-dependent hydrogen production, with maximum theoretical efficiencies of 10 − 13% and 6%, respectively (Ghirardi et al., 2009). However, there are still challenges to be overcome before industrial scale hydrogen production by phototrophic microbes becomes feasible. These include, the oxygen sensitivity of hydrogenases and nitrogen excluding nitrogenase, amongst others. Besides the above described oxygenic phototrophs, anoxygenic phototrophs, including green sulphur bacteria and purple sulphur and non-sulphur bacteria are also able to produce hydrogen photosynthetically under certain conditions (Chandrasekhar et al., 2015).

1.6 Microalgal wastewater treatment

In industrial scale microalgae cultivation, nutrients cost up to 10% of the total cultivation expense (Delrue et al., 2016). Therefore, it is reasonable to seek alternatives to synthetic nutrients. Microalgae have been reported to grow in multiple nutrient rich wastewater types. These include municipal wastewaters, anaerobic digestion reject waters, piggery and dairy wastewaters (Delrue et al., 2016). The wastewater type will limit the usage of the resulting biomass, as there are many

wastewater sources which are considered toxic, or at least harmful and would therefore be unsuitable for use in *e.g.* pharma and/or nutraceuticals (Lavrinovičs and Juhna, 2017).

Microalgal wastewater treatment can be seen as either an add-on (*e.g.* tertiary nutrient removal or polishing) or alternative to conventional biological wastewater treatment process. It offers several advantages as it has been demonstrated to remove phosphorous efficiently than the conventional biological wastewater treatment process and it also produces oxygen, which can be beneficial to other processes and may reduce the energy needed for aeration (Delrue et al., 2016).

1.6.1 Wastewater compositions

Typical municipal wastewater contains nitrogen and phosphorous as the main nutrients, which originate mainly from urine. Municipal wastewater can also contain some trace amounts of metals, including heavy metals and micropollutants (pharmaceuticals and other possibly toxic organic molecules). Characteristics of opaque wastewaters originating from agricultural activities are high nutrient concentrations and organic loading (Pittman et al., 2011), whilst high doses of salts, chemical toxins and heavy metals are typical for industrial wastewaters, which may contain only trace amounts of nitrogen and phosphorous (Delrue et al., 2016; Pittman et al., 2011). Municipal wastewater has been used for the publications presented in this thesis. Thus, microalgal nitrogen and phosphorous uptake were examined.

1.6.2 Nutrient uptake mechanisms

1.6.2.1 Nitrogen

In non-nitrogen fixing cyanobacteria and green algae, nitrogen uptake occurs mainly through specific membrane transporters and permeases (Flores and Herrero, 2005; Harris, 1989). Both prefer ammonium as the source of nitrogen and ammonium functions as a suppressor of nitrite and nitrate transporters. Notwithstanding, ammonium in high pH values and temperatures forms volatile ammonia gas that in turn inhibits the growth of both cyanobacteria and green algae by damaging the PSII complex (Collos and Harrison, 2014; Drath et al., 2008). Under adequate ammonium concentrations, ammonium transporters will use cellular ATP reserves to actively transport ammonium into the cells. When ammonium levels reach sufficient concentrations inside the cells, the transporters became deactivated (Collos and Harrison, 2014).

In the absence of ammonium, nitrate and nitrite transporters are activated. Nitrate is reduced to nitrite in the cytosol by the nitrate reductase (NR) enzyme. Nitrite, created by NR or taken up by a transporter, is carried over the chloroplast envelope in green algae (Sanz-Luque et al., 2015). Subsequently, nitrite is reduced to ammonium by nitrite reductase (NiR), located on the stromal side of the chloroplast in green algae and in the cytoplasm of the cyanobacterial cell. Eventually, cellular ammonium is used in amino acid synthesis (Flores and Herrero, 2005; Sanz-Luque et al., 2015).

1.6.2.2 Phosphorous

Phosphorous is the third largest cellular element after carbon and nitrogen and on average these are considered to be present in the ratio of 106:16:1 proposed by Redfield, (1934). As for fossil fuels, phosphorus is also a limited resource. Phosphorous is an important nutrient for agriculture, the reduction of which will have an impact on food security . It has been predicted that the phosphorus reserves will run out during next 30 or 300 years, this is why it is important to commence the recycling of phosphorus soon (Cordell and White, 2011).

Both cyanobacteria and green algae prefer phosphates as their source of phosphorous (Harris, 1989; Pitt et al., 2010). Besides this, they are able to utilize phosphorous from other sources, like organic phosphorous, through the use of specialized enzymes. Under phosphate-replete conditions, green algae express low affinity active transporters and store excess phosphates inside polyphosphate bodies that can be utilized when there is no phosphorus available for the cells (Harris, 1989; Ritchie et al., 1997). These polyphosphate bodies are shared between the dividing cells and in that way they work as phosphorous reservoirs for the daughter cells (Henry and Crosson, 2013).

In a study performed by Powell et al. (2009), they found that under moderate light intensity and phosphate concentration the green algal biomass accumulated over three percent of cellular biomass as phosphate. This phenomenon, where green algal cells accumulate phosphates beyond necessity, is called the luxury uptake of phosphorus.(Powell et al., 2009).

1.6.3 Microalgal wastewater treatment systems

The most common approach for the utilization of phototrophic microbes in wastewater treatment is the waste stabilization pond approach (Powell et al., 2009). In one to two meter deep facultative waste stabilization ponds (also known as the photosynthetic ponds), the upper layer consists of phototrophic microbes (Corley,

2011). Mainly, the species consists of green algae as they often dominate hyper-eutrophicated water bodies (Nair Aneesh et al., 2015). Underneath the oxygen evolving upper layer, there is a facultative layer. In this layer aerobic and facultative bacteria utilize the oxygen produced by photosynthesis and dissolved from the air, to oxidize the organic matter (Corley, 2011). The bottom layer consists of organic material that is degraded by anaerobic bacteria, yielding mainly CO_2 and methane (Corley, 2011).

Other microalgal wastewater treatment systems include high rate algal ponds (HRAP) and also closed photobioreactors (PBRs) (both described in section 1.4.), although these are not as common as waste stabilization ponds ((Lundquist et al., 2010;Delrue et al., 2016; Ho et al., 2017). Although there are benefits of a closed production system, the economics are not as attractive as open systems. This has thus far limited their popularity as conventional, stand-alone wastewater treatment systems (Xin et al., 2016).

1.7 The immobilization of phototrophic microbes

Photosynthesis allows the application of algae and cyanobacteria in the industrial production of different natural products (*e.g.* polyhydroxyalkanoates, carotenoids and nutraceuticals), with sunlight and CO_2 the only other raw materials required (at the time of writing, there are several examples of companies producing in this manner including: MIAL, Euglena Co, Ecoduna, AlgaEnergy, and AstaREAL). Importantly, photosynthetic microbes can also host novel production pathways and function as microbial cell factories to produce targeted chemicals and biofuels. However, general inherent problems of solar-based suspension production systems exist. These include: (i) self-shading leading to low light utilisation and a decrease production efficiency, (ii) excessive water consumption and (iii) energy intensive mixing. These problems drastically decrease the economic feasibility of microalgal based production platforms. To overcome the bottlenecks of suspension cultures, algal and cyanobacterial cells can be immobilized on different solid carriers, or entrapped within different matrices.

In nature, some algae and cyanobacteria naturally form biofilm structures by producing extracellular polymeric substances (EPS). These substances mediate the attachment of the cells towards each other (Laspidou and Rittmann, 2002). Benthic and lithotrophic strains produce protective EPS layers in every environmental condition (Little and Depalma, 2013), whereas planktonic strains have mostly been observed to produce EPS under certain stress conditions, such as nutrient starvation, pathogen and grazer attacks (Carney and Lane, 2014; Lampert et al., 1994).

Microalgal cells may also be immobilized to improve the efficiency of biofuel production processes (Kosourov et al., 2017; Leino et al., 2012), this can be done either passively or actively.

The passive approach to immobilization exploits the natural tendency of the cells to form biofilms. In this case, the cellular EPS mediates the attachment to a solid support, which is usually a positively charged material (de-Bashan and Bashan, 2010). In contrast to passive immobilization, active immobilization involves the cells being artificially confined using either physical or chemical methods (Vasilieva et al., 2016). The most commonly used approaches to active immobilization are gel entrapment and cell encapsulation. In gel entrapment, a porous matrix is applied to confine cell movement in respect to each other (de-Bashan and Bashan, 2010; Kosourov et al., 2018 B). In cell encapsulation, a semi-permeable membrane is formed around a single cell (Kosourov et al., 2018 B).

Of the aforementioned methods, gel entrapment is the most widely used method for whole cell immobilization. A broad spectrum of different materials have been employed in gel entrapment approaches. These include synthetic polymers, proteins and polysaccharides (chitin, agar, alginate, and nanocellulose, amongst others) (Jämsä et al., 2018;Kosourov et al., 2018 B; Vasilieva et al., 2016). The immobilization itself has various effects on a microalgae cell. For instance, the cellular chlorophyll content doubled in immobilized *Chlorella vulgaris* cells compared with suspended cells (Lau et al., 1998). However, the responses are dependent on species and materials used in the immobilization process (Vasilieva et al., 2016).

1.7.1 Advances in immobilization for photohydrogen production

The immobilization of photosynthetic cells offers several benefits for biohydrogen production. The most important enhancement, brought by thin layer immobilization, is the improvement of light utilization efficiency. As explained by Kosourov et al. (2018 B), suspension cultures have photoinhibition and shaded zones which are wider compared with the thin layer immobilized cells. The light harvesting efficiency value of the immobilized cells can increase to some extent compared to suspended cells (Kosourov and Seibert, 2009).

Another important feature of efficient thin layer immobilization is the cessation of cell division, this allows reductants to be directed more efficiently towards desired products (Kosourov et al., 2017). In addition, when the green algae are used for hydrogen production, immobilization makes the transition from sulphur-rich to

sulphur-deprived conditions more convenient (Eroglu and Melis, 2016). In these ways, immobilization has been demonstrated to prolong hydrogen production double for *Anabaena* cells (Leino et al., 2012) and over six-times for *Chlamydomonas* cells (Laurinavichene et al., 2006).

Interestingly, immobilization enables hydrogen production with sulphur/phosphorous-deprived cells even in the presence of atmospheric oxygen by protecting the cells from atmospherical oxygen (Kosourov and Seibert, 2009). Thin layer immobilization also enables precise engineering of light utilization efficiency through the layering of wild type and engineered strains. In this case, the top layers of films consist of mutant cells with truncated light-harvesting antenna and lower chlorophyll content, whilst the lower layers are wild type cells with higher chlorophyll content (Kosourov et al., 2018 B).

1.7.2 Immobilization using cellulose nanofibrils (CNF)

Of the previously listed materials, calcium crosslinked alginate is the most widely used material for the immobilization of microalgal cells. It is produced by brown algae and is a sticky and dense liquid material (Moreno-Garrido, 2008). For the immobilization of microalgal cells, it has several beneficial features, including: transparency, biocompatibility and ease of handling (Kanatt et al., 2018). However, it lacks some important features that are desired for microalgal cell entrapment. These include mechanical stability and high porosity (Jämsä, 2018). One example of a natural polymer exhibiting these desired properties is TEMPO-oxidized (2,2,6,6-tetramethylpiperidine-1-oxyl radical) cellulose nanofibrils (TEMPO CNF) (Saito et al., 2006). In TEMPO-oxidation, carboxylic groups are formed on the outermost hydroxyl groups. This facilitates the subsequent disintegration step of the individual nanofibers, yielding a transparent gel-like material with the desired mechanical strength and porosity (Saito et al., 2006). Indeed, it is already used as an immobilization and 3D-culturing matrix for mammalian cells (Liu et al., 2016).

2 AIMS OF THE STUDY

An increasing global demand for advanced biofuels has driven interest in microalgae as a suitable raw material. For microalgae to be considered feasible, conversion efficiencies must be improved. In this thesis, the suitability of a number of native strains isolated from the Finnish environment and some model strains of algae and cyanobacteria have been investigated for their potential use in biofuel production. Two approaches have been taken toward efficiency gains: the first is to couple biomass/biodiesel production with wastewater treatment; the second is to further improve light utilization of biohydrogen production through the employment of a novel approach to microalgal immobilization. Thus, the following objectives have been addressed in this thesis:

(i) To evaluate the capacity of native microalgal species for nutrient removal and lipid accumulation under low energy growth conditions in artificial wastewater (paper I)

(ii) To manipulate process parameters for integrated wastewater remediation and high lipid accumulation under Nordic climate conditions (paper II)

(iii) To evaluate the compatibility of TEMPO CNF as a suitable matrix for the immobilisation of microalgal cells for efficient photosynthetic hydrogen production (paper III)

3 METHODOLOGY

3.1 Cyanobacterial and green algal strains and storage conditions

Table 4. Cyanobacterial and green algal strains used in the study

Strain	Code	Paper	Reference
Synechocystis sp. (control strain)	PCC 6803	I	(Williams, 1988)
Chlorella vulgaris (control strain)	UTEX 265	I	(Kessler and Huss, 2018)
Synechococcus sp.	1TU21S5	I	(Rajaniemi-Wacklin et al., 2006)
Unknown	1TU44S8	I	N/A
Snowella litoralis	0TU37S4	I	(Rajaniemi-Wacklin et al., 2006)
Microcystis sp.	SYKE695	I	Personal communication, Lyudmila Saari
Scenedesmus sp.	UHCC0027	I & II	(Lynch et al., 2015)
Synechococcus sp.	1TU39S1	I	(Rajaniemi-Wacklin et al., 2006)
Synechococcus sp.	0TU24S4	I	Personal communication, Anne Ylinen
Microcystis sp.	SYKE2088A	I	Personal communication, Lyudmila Saari
Anabaena sp. Δ*hupL*-mutant	PCC 7120	III	(Masukawa et al, 2002)
Chlamydomonas reinhardtii	CC-124	III	(Pröschold et al., 2005)

The *Synechocystis* sp. and *Chlorella vulgaris* control strains were acquired from the Pasteur Culture collection of Cyanobacteria (PCC) and the UTEX Culture Collection of Algae at the University of Texas at Austin, respectively. All Finnish native strains used in papers I & II were obtained from the University of Helsinki Culture Collection (UHCC). Prof. H. Sakurai (Waseda University, Japan) provided the Δ*hupL*-mutant of Anabaena sp. PCC 7120. This mutant lacks the large subunit of the [Ni–Fe] uptake hydrogenase enzyme (accession no. AAC79878.1), resulting in increased hydrogen production rates. *Chlamydomonas reinhardtii* strain CC-124 (mt−, nit−) was obtained from the Chlamydomonas Resource Center at the University of Minnesota, USA.

All strains were maintained under continuous low light (approximately 15 μmol photons m^{-2} s^{-1}, photosynthetic active radiation (PAR), cool-daylight, Lumilux T8 15W/865) at room temperature, approximately 22 °C. The strains used in papers I & II were kept in standard BG11 medium, buffered with 5 mM HEPES (pH 7.4). The *Anabaena* sp. Δ*hupL*-mutant used in paper III was stored in Z8x medium (Kotai, 1972), where x denotes the absence of combined nitrogen. *Chlamydomonas reinhardtii* was stored in standard Tris-Acetate-Phosphate (TAP) medium (Harris, 1989).

3.2 Pre-culture and experiment growth conditions

Pre-cultures were generally cultivated under the conditions of the experiment, which followed. In work presented in papers II & I, synthetic wastewater was used. This was modified from regular BG11 medium according to Shi et al. (2007). Concentrations of nitrate-N (NO_3^--N) as $NaNO_3$, ammonium-N (NH_4^+-N) as NH_4Cl, and phosphate-P (PO_4^{3-}-P) as K_2HPO_4 were approximately 3, 21, and 4 mg L^{-1} respectively. The pH was buffered to 7.4 with 5 mM HEPES and autoclaved prior to use. For experiments employing real municipal wastewater, the NH_4^+-N and PO_4^{3-}-P concentrations of the synthetic pre-growth media were adjusted to have concentrations equal to the real municipal wastewater of the experiments (average values of 42 mg L^{-1} and 5 mg L^{-1}, respectively).

For the screening described in paper I, ten unicellular cyanobacterial and green algal strains (section 2.1) were grown in synthetic wastewater in 500 mL batch cultures (starting OD_{750nm} 0.1) under 40 μmol photons m^{-2} s^{-1} light intensity (continuous), at 22 °C and mixing at 100 rpm for 14 days (Lynch et al., 2015). Culture parameters, which were followed, include: OD_{750nm}, chlorophyll a, NH_4^+-N and PO_4^{3-}-P (methods are detailed in section 3.3).

The experiment included an unseeded blank sample. The blank value was removed from corresponding measured values and the nutrient removal was calculated using (equation 5):

$$\%\text{-removal}(t) = 100\times(([b]t-[s]t)/[b]t)) \quad \textbf{(Equation 5)}$$

where t is time, b is the method blank, and s is the sample.

Prior to the optimization of growth conditions presented in paper I, tolerance to high light (500 µmol photons m^{-2} s^{-1}) and high CO_2 (3% CO_2) were tested in 24-well plates over a four-day growth period, with OD_{750nm} and Chlorophyll a indicative parameters (section 2.3). Lab-scale optimization of growth and nutrient removal was subsequently performed for strain UHCC0027 algal cells (table 4) through use of high (3%) CO_2 conditions in both synthetic and real wastewater (paper I). Experimental conditions were the same as in the screening test, but a light:dark cycle of 16:8 hours was used under a higher light intensity of 220 µmol photons m^{-2} s^{-1}. Only ammonium and phosphate concentrations were measured, which had starting values of 42 mg L^{-1} and 5 mg L^{-1}, respectively. All real wastewater employed in the work originated from the Varissuo district of Turku, (Finland).

In the pilot-scale study presented in paper II, the UHCC0027 alga was grown in 5-liter Erlenmeyer flasks with an aeration rate of 4 L min^{-1} in the artificial municipal wastewater already described. The pre-culture period was ten days under a light intensity of 225 µmol m^{-2} s^{-1} of PAR (14:10 hour (light:dark) photoperiod). Ambient temperature cultures were grown at 22 °C and the cold temperature experiment pre-culture was grown at 6 °C. Five experiments, including two unseeded control experiments, were then performed in 24-liter reactors (Fig. 3) using real municipal wastewater (Varissuo district of Turku, Finland). Experimental conditions are summarized in Table 5.

Table 5. Pilot-scale experimental conditions in PBRs for wastewater of the composition: High COD, Low nutrient (HC_LN); Low COD, High nutrient (LC_HN); and Low COD, High nutrient operated under cold temperature (LC_HN cold). Values marked NM were not measured. COD stands for chemical oxygen demand.

Wastewater type and experimental conditions	High COD, Low N (HC_LN)	Low COD, High N (LC_HN)	Low COD, High N under cold temp. (LC_HN cold)
Reactor volume	24 L	24 L	24 L
Light period and intensity	14:10 light/dark, 250 µmol m^{-2} s^{-1}	14:10 light/dark, 250 µmol m^{-2} s^{-1}	14:10 light/dark, 250 µmol m^{-2} s^{-1}
Temperature	16−26 °C, average 22.8 °C	22−29 °C, average 25.5 °C	7−13 °C, average 8.3 °C
Aeration	0.625 v v^{-1} min^{-1}	0.625 v v^{-1} min^{-1}	0.625 v v^{-1} min^{-1}
NH_4^+-N (mg L^{-1})	42	56	56
NO_3^--N (mg L^{-1})	0.4	0.4	0.4
NO-N (mg L^1)	< 0.15	< 0.15	< 0.15
Total-N dissolved (mg L^{-1})	NM	59	59
PO_4^{3-}-P (mg L^{-1})	4.5	5.4	5.4
Total-P dissolved (mg L^{-1})	NM	6.1	6.1
N:P (molar ratio)	20.6	22.9	22.9
COD dissolved (mg L^{-1})	490	84	84
COD-total (mg L^{-1})	560	600	600

The pre-grown cells, described earlier, were harvested by centrifugation (6000 ×g, 10 min). The cell amount in reactors was adjusted to approximately 1.6×10^6 cells mL^{-1}, determined by cell counting using a Bürker hemocytometer.

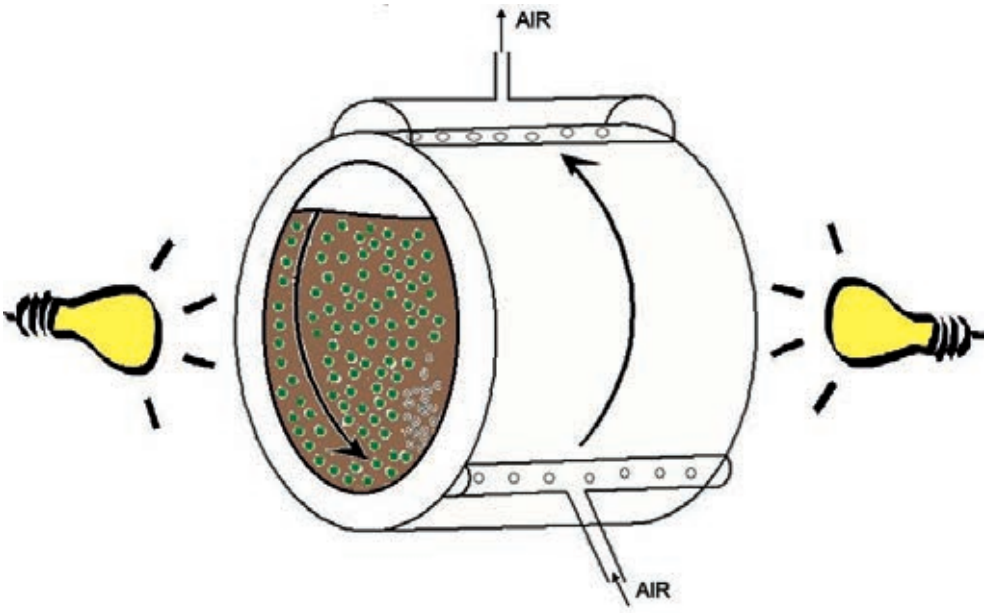

Figure 4. Schematic illustration of the 24-liter photobioreactor (PBR) used in the pilot-scale studies.

The first experiment was performed during springtime (April, morning) and the wastewater was collected after pre-screening from a municipal sewer line. Characteristic of this wastewater batch was a high COD concentration and lower nutrient concentrations denoted as HC_LN. The second experiment was performed during summertime (June – July, afternoon) and characteristic of that batch was low dissolved COD concentration and a higher nutrient concentrations denoted as LC_HN. In addition to the ambient temperature experiments, a colder temperature experiment (7 – 13 °C), denoted as LC_HN cold, and was run with the same wastewater batch as the LC_HN experiment.

Clewer Oy (Turku, Finland) provided the reactors, which had a horizontal cylinder shape, with 40 cm diameter and 20 cm length (figure 4). Reactors had a perforated stainless steel internal wall with multiple small holes, facilitating the even distribution of nutrients and cells. The reactors were mixed by aerating at a rate of 0.625 v v^{-1} min^{-1}. At both ends of the reactor, one 125 W CFL-Lamp (LUMii, UK, color temperature 6400 K) was placed at a distance of 10 cm from the transparent reactor windows. Light intensity, measured from inside of the reactor, right next to the transparent window, was 250 µmol m^{-2} s^{-1}. Ambient and liquid phase temperatures were measured using a Fluke 54II thermologging device.

The work presented in paper III involved growth of the *Anabaena* sp. Δ*hupL*-mutant in Z8x medium under constant 60 µmol photons m^{-2} s^{-1} light at 26 °C. The *Chlamydomonas reinhardtii* strain used in the same study was grown in the same way as the *Anabaena* sp. Δ*hupL*-mutant, but standard Tris-Acetate-Phosphate (TAP) medium was used. Both cultures were aerated with sterile air, which was filtered through Acro 37 TF (Gelman Sciences, USA) filters.

3.3 Biomass and nutrient measurements

Biomass accumulation was generally determined using OD measured spectrophotometrically at 750nm. For work presented in paper II, dry weight was measured according to APHA method 8111G, with a drying temperature of 105 °C and a 1.2 µm pore size filter (Whatman GF/C,). The chlorophyll a content of cyanobacteria was determined according to (Lichtenthaler, 1987) (Paper I, II). Briefly, a known amount of cell culture was centrifuged and the chlorophyll was extracted in 90% methanol solution at 65 °C for 20 minutes. Absorbance was then measured with a spectrophotometer (665 nm). The total (a+b) chlorophyll content of green algae was measured according to (Porra et al., 1989) in 100% methanol (paper II) or according to the method introduced in the Chlamydomonas Sourcebook (Harris, 1989, paper III). For paper I, ammonium and phosphate concentrations were followed using Spectroquant® photometric test kits (Merck, 100683 and 114848, respectively), according to the manufacturer protocols. Hach Lange LCK cuvette tests were used to measure nutrient and COD concentrations in the study presented in paper II (NH_4^+-N, NO_2^--N, NO_3^--N, and total-N, PO_4^{3-}-P, total-P, and COD).

3.4 Photosynthetic activity monitoring

The effective photosystem II yield, Y(II), and light response curves of Y(II) were measured using a DUAL-PAM 100 fluorometer (Walz, Effelrich, Germany) from samples which had chlorophyll a concentration adjusted to 5 µg mL^{-1}.Y(II), was calculated with the following formula (equation 6):

$$Fm' - Ft / Fm' \qquad \textbf{(Equation 6)}$$

Here, Fm′ is the maximum fluorescence level in light, obtained by firing a saturating light pulse (300 ms/3000 µmol photons m^{-2} s^{-1}) to illuminated cells. Ft is the steady-state chlorophyll a fluorescence level, determined during the illumination of the cells with actinic red light intensity of 126 µmol photons m^{-2} s^{-1}. Light response curves of

Y(II) were recorded during the step-wise increase of light intensity form 0 to 829 μmol photons m^{-2} s^{-1}, with a 30 s illumination at each step.
In paper III, (YII) was presented as measured by a PAM-2000 (Walz, Germany) fluorometer. In this case, the maximum fluorescence level (Fm′) at light was obtained by firing a saturating light pulse (800 ms/2000 μmol photons m^{-2} s^{-1}) to the cells. The steady-state Chl a fluorescence level (Ft) was determined with red actinic light of 84 μmol m^{-2} s^{-1}.

3.5 Determination of neutral lipid contents

The neutral lipid screening presented in paper I was performed using BODIPY (4,4-difluoro-1,3,5,7,-tetramethyl-4-bora-3a,4a-diaza-s-indacene) (505/515) lipophilic dye detected by e flow cytometry. Data obtained from measurements was collected using FACSDiva software v. 6.1.3, followed by analysis with Flowing software v.2.5 (http://www.flowingsoftware.com)) as detailed in Lynch et al. (2015).

The total lipid content of cells was also measured gravimetrically, according to the method of Ryckebosch (et al., 2012). Lipids from approximately 10 mg of lyophilized biomass were extracted over several steps. Initially, 400 μl of methanol was added to the biomass and vortexed. Chloroform (200 μL) and MQ-water (40 μL) were then added and the mixture was again vortexed. Finally, chloroform (200 μL) and MQ-water (200 μL) were added, followed by vortexing and centrifugation (2000 rpm, 10 min). The oleaginous layer was removed and passed through a column containing anhydrous sodium sulfate to dry any remaining water. The organic solvent phase was then evaporated using a heating block at 40 °C. The sample was kept under under continuous nitrogen flow to prevent oxidation of the lipids. Following this procedure, the obtained pellet was again extracted with chloroform:methanol 1:1 (400 μL) and MQ-water (120 μL). The masses of lipid obtained following both extractions were summed to give the total lipid content per cell dry matter.

3.6 Fatty acid composition and the prediction of biodiesel properties

Lipid analysis (both total-lipids and FAME composition) was performed for the LC_HN and LC_HN cold experiments presented in paper II. The first sample was taken on the final day of the pre-growth period and the following samples at days five and ten for the ambient-temperature experiments. For the colder-temperature experiment, the sampling days were: 0, 14 and 28. Prior to lipid analysis, the samples

were vacuum-filtered through 20 μm nylon membrane filters to remove larger debris (Sterilitech, USA). The filtrate was centrifuged (6000 ×g, 10 min) to obtain a biomass pellet, which was snap frozen in liquid nitrogen. The last step before lipid analysis was lyophilization of the biomass using a Flexi-dry μP (FTS systems, USA) freeze dryer.

In order to determine the fatty acid profile of each sample, in situ transesterification was performed according to Van Wychen and Laurens (2013). An Agilent 7890C gas chromatograph connected to a 5975C inert mass detection unit was used with an Agilent Innowax 19091N-213 (30 m× 0.32 mm× 0.5 μm) column. One microliter of sample was injected in splitless mode, with Helium as carrier gas (1.4 mL min^{-1}). The separation of FAMEs was performed using a gradient program (50 °C for 8.5 min, ramping to 250 °C at 15 °C min^{-1}, and a final hold at 250 °C for 8 min). A FAME mixture, consisting of 37 different FAMEs (18919-1AMP, Supelco) was used as a standard. The FAMEs were quantified using protocols described by Devle et al. (2009), Van Wychen and Laurens, (2013). The C16:4 FAME was an exception, as it was quantified using the 4(Z), 7(Z), 10(Z), 13(Z)-hexadecatetraenoic acid-d_5 standard (C16:4, Cayman Chemical) which was transesterfied using the same protocol. The esterification efficiency was determined using stearidonic acid and stearidonic methyl ester standards (C18:4 FA and C18:4me, Cayman Chemical). Biodiesel properties were predicted by applying the formulas reported by Talebi et al. (2014). Only the oxidative stability was estimated separately, according to the formula developed by (Park et al., 2008).

3.7 Determination of H_2 and O_2 contents

In paper III, H_2 and O_2 concentrations were presented as measured from inside of gas tight vials. Samples of 150 μL were taken using a gas-tight 250 μL gas chromatography syringe (Hamilton, USA) equipped with a sample lock. The samples were injected into a Clarus 500 gas chromatograph (PerkinElmer, Inc.) equipped with a thermal conductivity detector and a molecular sieve 5 A column (60/80 mesh) in order to determine concentrations.

3.8 Materials used in immobilization studies

All chemicals were of analytic grade and used as received. 2,2,6,6-Tetramethylpiperidin-1-oxyl (TEMPO), sodium bromide (solid),10% sodium hypochlorite (aqueous) and $CaCl_2$ (99%, #C7902) were purchased from Sigma-Aldrich and 0.1 M sodium hydroxide solution was obtained from Fluka Analytical.

Ultrapure water (MQ-water,18.2 MΩ cm) was made with a Milli-Q purification unit (QPAK® 1, Millipore).
TEMPO-oxidized cellulose nanofibrils (TEMPO CNF) were prepared using undried bleached softwood pulp (a spruce/pine mix) obtained from a Finnish pulp mill as the raw material. TEMPO-mediated oxidation of the pulp fibers was performed according to Saito et al. (2006).

Polyvinyl alcohol (Mowiol 56-98, Mw 195 000 g mol-1, DP 4300, Sigma-Aldrich) was used as a CNF film wet strength additive. It was diluted to a 5 wt% solution with Milli-Q water at 95 °C. Branched polyethylene imine (PEI, Mw 70 000 g mol^{-1}, 30 wt% aqueous solution, Polysciences) used as the anchoring polymer for CNF thin films and used as received. Alginate (#71238, Sigma-Aldrich), originating from brown algae, was used for immobilization as a 4 wt% solution, made up using MQ-water and sterilized by autoclaving at 121 °C for 10 min.

3.9 Immobilization techniques

In paper III, three different approaches to immobilization were undertaken (A, B and C). A detailed schematic illustration of the approaches, described below, is presented in paper III, as figure 2.

In approach A, *Anabaena* sp. Δ*hupL*-mutant cells were entrapped within thin hydrogel layers. These layers were formed on top of a blotting paper support (3MM Chr, #3030-931, Sigma-Aldrich). Wet cell pellets were first mixed 1 : 1 wet-mass ratio with different hydrogels: (i) 1 wt% TEMPO CNF; (ii) 1 wt% TEMPO CNF and 0.1 wt% polyvinyl alcohol (PVA); and (iii) 4 wt% alginate as a control. In this study, PVA was added to the second formulation to see the possible effects, as it was needed in further studies as a crosslinking chemical. The layers were formed on a top of blotting paper by drawing down the formulations with a stainless steel rod along the paper to produce uniform layers. Following this, the layers were cut into 3 × 1 cm strips and placed on top of 3 × 1 × 1 cm melamine foam sponges, which provided water for the strips. Finally, these constructs were placed inside 33 mL gas-tight vials filled with 5 mL of Z8x medium. The vials were filled with argon containing 6% CO_2 and placed at 26 °C under a light intensity of 140 µmol photons m^{-2} s^{-1} PAR. To enable comparisons with previous studies performed with alginate strips, Ca^{2+}-crosslinking was applied to alginate polymers in all immobilization approaches.

In approach B, *C. reinhardtii* cells were pre-treated under sulfur-depleted conditions to initiate H_2 photoproduction (Melis et al., 2000). Briefly, algal cultures were grown to late logarithmic phase (~25 µg total chlorophyll per mL), Cells were centrifugated

(3000 g for 3 min) and the pellet washed in TAP-minus-sulfur-minus phosphorus (TAP-S-P) medium to remove sulfates and phosphates. The pelleted cells were entrapped within TEMPO CNF hydrogel layers by the method of Kosourov and Seibert (2009) for alginate strips. In this method, a white-polymer insect screen was attached to the sticky side of a Scotch-type tape and the cells mixed with matrices were smeared over this structure. The cellular and TEMPO CNF hydrogel or alginate formulations were mixed in 1 : 1 wet mass ratio with (i) 0.5 wt% TEMPO CNF, (ii) 0.5 wt% TEMPO CNF + 0.05 wt% PVA and (iii) 4 wt% Ca^{2+}-alginate as a control. In contrast to approach A, both TEMPO CNF and alginate hydrogel matrices were stabilized by spraying the surface with 50 mM $CaCl_2$ solution and allowed to stabilize for 20 minutes before washing with MQ-water. Finally, strips were cut (6 × 1 cm) and submerged in 10 mL TAP-S-P medium inside 75 mL gas-tight vials filled with Argon gas. The vials were placed horizontally under a light intensity of 50 µmol photons m^{-2} s^{-1} PAR at 26 °C.

In approach C, the PVA-crosslinked TEMPO CNF films were prepared exactly in the same way as in approach A. However, the crosslinking with PVA was achieved by drying the films on the top of the paper support for 22 h, in complete darkness at 23 °C and 70% relative humidity. The hydrogel formulations consisted of wet biomass mixed in either a 1:1 or 1:2 mass ratio with 0.5 wt% TEMPO CNF and 0.05 wt% PVA as a crosslinker. Dried 4 wt% Ca^{2+}-alginate films served as a control. In addition, the matrix-free cell biomass placed on top of the paper support served as a negative control.

The dried cells were recovered by placing the cells under a mild growth condition. In this recovery approach, the films and the supporting blotting paper were placed on a top of a melamine foam sponge, which supplied Z8x medium to the entrapped cells. The film on top of the paper support and sponge was placed inside a closed, but not sealed, Petri dish at 26 °C under an air atmosphere supplemented with 0.5% CO_2, with 6 µmol photons m^{-2} s^{-1} PAR light intensity. The cells were recovered under these conditions for four days. After this recovery period, the film-coated paper was cut into 3 × 1 cm strips and hydrogen producing conditions were the same as in approach A.

3.10 QCM-D

The surface interactions between *Anabaena* sp. Δ*hupL*-mutant cells and TEMPO CNF and PEI coated TEMPO CNF were investigated with Quartz Crystal Microbalance with Dissipation Monitoring (QCM-D) using the Q-Sense E4

instrument (Q-SenseAB, Gothenburg, Sweden), which allows direct application of desired sample solutions onto the sensor surface. AT-cut quartz crystal sensors with gold electrodes, used in QCM-D experiments, were purchased from Q-sense AB (Gothenburg, Sweden), with a fundamental resonance frequency of 5 MHz and a sensitivity constant reported by the supplier. The detailed protocol is presented in paper III and in the corresponding electronic supplementary material.

3.11 Statistical analysis

Wherever possible, samples were analyzed in duplicate or triplicate and data presented as the mean of replicates with the relevant standard deviation. Please refer to individual publications for details of replicates for particular experiments. Where significance between results has been discussed, student t tests have generally performed. Details of significance testing can also be found in the individual publications.

4 OVERVIEW OF THE RESULTS

4.1 Screening for the most efficient microalgal strain: nutrient removal and biomass accumulation

For the first paper, screening of strains for efficient biomass accumulation and nutrient removal was performed using synthetic wastewater. Eight different unicellular, non-toxic phototrophic microbes were selected from the University of Helsinki Culture Collection. A unicellular nature was desired based on the suitability of cells to rapid neutral lipid detection using flow cytometry. *Synechocystis* sp. PCC 6803 and *Chlorella vulgaris* served as reference cyanobacterium and green alga strains, respectively.

Experiments were performed under low energy conditions (40 µmol photons m^{-2} s^{-1} continuous light, 22 °C and mixing at 100 rpm) and the lag phase lasted approximately four days for most of the isolates (Paper I, Fig 1.). During the 14-day growth period, the UHCC00027 isolate clearly stood out from the other strains based on the OD_{750nm} increase and phosphate removal (Paper I, Fig. 1 A & D). In chlorophyll a accumulation, the ITU44S8 strain outperformed other strains, this was noticeable during the final two days of the experiment (Paper I, Fig. 1 B). However, none of the strains demonstrated efficient ammonium removal (none removed more than 50% of the starting concentration).

As high CO_2 concentration and light intensity is known to enhance biomass accumulation rates, and thus presumably nutrient removal, these conditions were used to optimize the experimental conditions. A test performed in 24-well plates with 3% CO_2 and 500 µmol photons m^{-2} s^{-1} (continuous light) light intensity demonstrated that the UHCC00027 again stood out from the rest of the strains (Paper I, Fig. 2). This was particularly evident under the high light condition where dilute starting concentrations were used. Indeed, under high CO_2 conditions, both green algae showed higher OD_{750nm} and chlorophyll a accumulation whereas the seven

cyanobacterial strains showed only moderate growth. Only the SYKE 695 cyanobacterium failed to grow under the high CO_2 and high light conditions.

4.2 Identification of UHCC0027

As the UHCC00027 isolate was the most efficient strain across many parameters, it was identified by sequencing approximately 3.4 KB of the 18S and ITS1 regions of its genome. Phylogenetic analysis using the NCBI database placed the UHCC00027 strain in the Scenedesmaceae family (Paper I, Fig. 7).

4.3 Comparing the growth of UHCC00027 cells in high and low CO_2 conditions in both synthetic and real wastewater

As the UHCC00027 isolate was most promising strain over several conditions, further studies were performed with that isolate. To validate the performance of UHCC00027 under relevant conditions for nutrient removal, real municipal wastewater was applied in an experimental set-up together with high and low carbon conditions.

The shift from a low carbon concentration condition to a high carbon concentration had the most dramatic effect on all of the measured parameters. Both phosphate and ammonium were removed by 90% after only three days of growth in real and artificial wastewater, whereas low carbon conditions meant removal did not exceed 70% for either nutrient (Paper I, Fig. 3). The ammonium removal rate was increased over five times faster in municipal wastewater and over eight times faster in synthetic wastewater when grown in high CO_2 conditions compared with low CO_2 conditions. In turn, the phosphate removal rate was increased over three times in municipal wastewater and over five times in synthetic wastewater. The OD_{750nm} and chlorophyll a readings increased to significantly higher levels in real municipal wastewater, likely due to the higher starting concentration of ammonium.

Clear drops in chlorophyll a concentration and phosphate removal occurred around day eight in the low carbon municipal wastewater culture (Paper I, Fig. 3 B & D). These drops were relative to the real wastewater blank control, which started to grow indigenous phototrophs around the same time.

The photosynthetic performance of UHCC00027 cells was monitored by determining the effective PSII yield (Y(II)) as a function of both time and light intensity (Paper I, Fig. 4) over the course of the five-day experiment. In both synthetic and municipal wastewater cultures, Y(II) values increased from initial values in the first two days (Paper I, Fig. 4 A). In synthetic wastewater Y(II) increased from 0.47 (±0.04) to 0.59 (±0.00) within 48 hours, whereas in municipal wastewater the increase was from 0.60 (±0.02) to 0.70 (±0.02) within 28 hours. After these time points, values progressively decreased to 0.27 (±0.05) and 0.36 (±0.02) for synthetic and municipal cultures, respectively.

4.4 Determination of neutral lipid content

For the rapid determination of neutral lipid content, strains were stained with BODIPY (505/515) fluorescent dye. Subsequently, specific fluorescent signals were detected using flow cytometry. Both green algae demonstrated significantly higher median fluorescence intensities (MFI) than the cyanobacterial isolates. These values were 1390 (±70) for UHCC00027 cells and 1220 (±120) for *Chlorella vulgaris* cells (Paper I, Fig. 5). Isolate 1TU44S8 had the highest cyanobacterial MFI signal of 764 (±102). The flow cytometry approach proved a rapid and sensitive technique. It was however, difficult to separate the specific signal from noise in the 0TU37S4 cell sample, likely due to extracellular polymeric substances located around the cells. However, washing the cells twice with 1 × PBS buffer alleviated this problem.
The total-lipid content of the two algal strains was also determined gravimetrically. For UHCC00027 cells, the total-lipid content was 23.45 (±0.61) and for *Chlorella vulgaris* it was 19.49 (±1.18) percentage lipids per dry weight. This reflected the same order of lipid content obtained using flow cytometry.

4.5 Pilot-scale experiments: nutrient removal and biomass accumulation

As the UHCC00027 strain was shown to be the most promising candidate for wastewater treatment and biofuel production, further pilot-scale studies were performed with it. In the pilot study, 24-liter photobioreactors were used to grow UHCC00027 cells in real municipal wastewater. A detailed breakdown of the composition of municipal wastewater used for the separate reactors is in table 5 (material and methods section 3.2). Briefly, the HC_LN reactor had higher dissolved COD concentration (490 mg L^{-1}) and lower nitrogen concentration (43 mg L^{-1} dissolved inorganic nitrogen), whereas the LC_HN reactor had lower dissolved COD concentration (84 mg L^{-1}) and higher nitrogen concentration (57 mg L^{-1} dissolved

inorganic nitrogen). The LC_HN cold reactor had the same wastewater composition as the LC_HN reactor but it was placed in cold room with average temperature of 8.3 °C. During the experiments, samples were taken for nutrient, biomass and lipid analysis.

4.5.1 Performance of UHCC0027 under Nordic summer temperatures

The wastewater used to fill the reactors was obtained in different seasons and at different times of the day. As such, the COD (chemical oxygen demand) and nutrient composition varied. The higher COD and lower nitrogen (HC_LN) wastewater COD concentration was 493 mg/mL compared to only 83.6 mg/mL in the lower COD, higher nitrogen (LC_HN) wastewater. However, the high COD observed decreased to the same levels of the LC_HN reactor within just one day. This rapid decrease was likely performed by fast-acting heterotrophic bacteria (Paper II, Fig. 2A), supported by the strong initial peak in the biomass accumulation curves of both the HC_LN seeded and HC_LN unseeded (blank) reactors (Paper II, Fig. 2C).

The UHCC0027 cells seeded in the HC_LN wastewater PBR demonstrated higher chlorophyll per volume, indicating faster growth than in LC_HN at ambient temperature. Over six days of growth, chlorophyll accumulation was 17% faster in the HC_LN experiment (Paper II, Fig. 1A) than in the LC_HN experiment. In both PBRs (LC_HN, HC_LN), the cells reached exponential growth in three days. The faster growth rate may have been due to the higher COD concentration in the HC_LN culture. Despite the fact that available nitrogen was depleted at the end of both seeded (LC_HN, HC_LN) experiments, chlorophyll concentrations did not reach stationary levels, with increases observed up until the final days of the experiments (Paper II, Fig. 1A).

Ammoniacal nitrogen was the major form of nitrogen present in the municipal wastewater (80% of total dissolved N) (Paper II, Table 5). In both HC_LN and LC_HN experiments higher rates of ammoniacal nitrogen removal were seen over the unseeded experiments. In seeded experiments, the average daily removal rates were for HC_LN and LC_HN experiments 7.6 and 6.7 mg L^{-1} d^{-1}, respectively. For the unseeded experiments the corresponding values were 4.3 and 2.4 mg L^{-1} d^{-1}. This suggests that processes other than microalgal ammonium uptake played more significant roles in ammoniacal N removal. The sudden drops in ammoniacal nitrogen concentrations (day one and two) are likely explained by ammonia air stripping. Whereas, after the fourth day of experiments, the nitrification process started play a role in ammoniacal nitrogen removal, seen in the pH drop and nitrate

and nitrite concentration increases (Paper II, Fig. 2B&S4). Nitrification rates were higher in the LC_HN reactors, which was likely caused by the higher temperatures and substrate concentrations (Paper II, Fig. S2). From the nitrate and nitrite data, it can be inferred that the nitrifying bacteria removed most of the ammoniacal nitrogen in the ambient temperature experiments. However, based on dissolved inorganic nitrogen (DIN) data plotted against the accumulation of algal biomass (Paper II, Fig. 3A), the positive contribution made by seeded and indigenous algae can also be seen.

Seeding with UHCC00027 cells was necessary to achieve over 90% phosphate removal in the experiments. For example, the blank HC_LN experiment had a rising phosphate concentration for most of the experiment. Only the growth of wastewater indigenous phototrophs in the very last days resulted in a final phosphate concentration, which was lower than the starting concentration. Besides the higher chlorophyll growth, also a 36% faster phosphate removal rate occurred in the HC_LN experiment.

Due to higher nitrogen and phosphorous concentrations in LC_HN experiment, total dissolved N and P concentration were followed to confirm the fulfillment of EU Urban Waste Water Treatment Directive (UWWTD) 91/271/EEC. UWWTD requirement for 10,000 – 100,000 population equivalent, 15 mg/L total N and 2 mg/L total P. The total dissolved nitrogen decreased from 55.8 mg/mL to 2.4 mg/mL within 12 days and the requirements of the UWWTD was fulfilled within ten days (Paper II, Fig. 2D & F).

4.5.2 Performance of UHCC0027 under Nordic spring and autumn temperatures

To test the performance of UHCC0027 cells under conditions occurring mostly during Finnish spring and autumn time, an experiment was performed in corresponding conditions (average temperature 8.3 °C and light intensity of 250 µmol m^{-2} s^{-1}). The light conditions were kept the same as the ambient temperature reactors (22.8 °C and 25.5 °C in the HC_LN and LC_HN experiments, respectively), so the effect of temperature alone could be evaluated. The cold temperature had dramatic effects on many parameters, including nutrient removal and biomass accumulation (Paper II, Fig. 1 & 2).

In cold conditions, the growth of the algae was slower and based on chlorophyll and dry weight measurements, exponential growth was reached around the 17th day of the experiment. Interestingly, during the exponential growth phase (from day 12 to 21); the biomass accumulation was only 22% slower than in the exponential growth

phase of the LC_HN experiment (Paper II, Table S1). The growth of phototrophic cells may originate from wastewater indigenous cells that appeared also in ambient temperature blank culture, confirmed by microscopy observation (Paper II, Fig. 1B & S3).

The effect of wastewater indigenous phototrophs can also be seen in phosphorous removal curves (Paper II, Fig. 2E & F) over days 15 – 20. Of particular note was the maximum rate of phosphate removal, which reached a higher maximum value in colder conditions compared with the room temperature experiment. A higher N:P ratio in the cold reactor was likely the main factor in the higher removal rate.
Overall, these findings showed the robustness of UHCC0027 cells to perform wastewater treatment under various conditions. The cold temperature experiment fulfilled the requirements of the UWWTD within 20 days. This is notable since ammonia air stripping and nitrification processes are significantly lower at low temperatures (Arogo et al., 1999; Saad and Conrad, 1993).

4.6 Biodiesel potential of UHCC00027 cells grown in real municipal wastewater

To investigate the suitability of UHCC00027 cells for integrated wastewater treatment and biofuel production, we included the detailed lipid analysis in the study. The lipid studies included determination of total lipid contents, FAME profiles and the prediction of biodiesel properties. Samples were taken from LC_HN experiment at three different growth phases, beginning, mid and late exponential growth phase.

4.6.1 Total-lipid contents

In room temperature experiments the total-lipid content increased along the duration of the experiments as the lipid contents were 16% and 18% in the beginning and mid growth phase (Paper II, Fig. 4 A). At the last measurement point, the total lipid content reached 47% of dry weight, which was the highest number met in this study. In contrast, the total-lipid contents did not vary as significantly under colder temperatures as the maximum content reached 34% of dry weight in the mid growth phase. When measured in the beginning, the content was 22% and at the end of the experiment, it was 33%.

4.6.2 FAME profiles

UHCC00027 cells had a reasonably similar FAME profiled compared with many green algae including *Chlamydomonas*, *Chlorella*, and *Scenedesmus* (Schwenk et al., 2013; Teoh et al., 2013). In all of the UHCC00027 seeded cultures the palmitate (C16:0) and α-linolenate (C18:3) fatty acids were the most abundant (Paper II, Fig. 4B & C). The highest percentage value of individual fatty acid was seen in the late exponential growth phase of the UHCC00027 in LC_HN PBR, when the percentage of α-linolenate reached 38% of fatty acid content. The most significant difference between room and cold temperature cultures was seen in the mid exponential growth phase when the saturated fatty acids were highly expressed in room temperature culture. Besides, the palmitate was more abundant in all of the room temperature growth phases. Another interesting feature is the appearance of the omega-3 fatty acid eicosapentaenoic acid (EPA, C20:5) both in cold temperature and blank reactor, presumably originating from wastewater indigenous algae (Paper II, Fig. S3).

4.6.3 Biodiesel properties

The biodiesel properties of the FAME mixtures were predicted using the BiodieselAnalyzer© tool (Talebi et al., 2014). Only the oxidative stability was predicted according to Park et al. (2008). The UHCC00027 cells appeared to have the typical properties of biodiesel obtained from green algal biomass (Stansell et al., 2012). The high unsaturation degree caused low cetane values and oxidative stability in most of the samples (Paper II, Table 2). As unblended fuels, none of the samples met the requirements of the US or EU standards for biodiesel.

4.7 Immobilization of phototrophic microbes in cellulose nanofibrils for the efficient production of biohydrogen

The immobilization of phototrophic microbes has several benefits in a multitude of applications. For instance, in wastewater treatment it facilitates the harvesting step and protect cells from stress caused wastewater environment (Kosourov et al., 2018 B; Vasilieva et al., 2016). In hydrogen production, immobilization improves light utilization efficiency and eases the sulphur deprivation step required for hydrogen production by green algae (Eroglu and Melis, 2016; Kosourov et al., 2017).

In the final work of this thesis, the suitability of TEMPO-oxidized (2,2,6,6-tetramethylpiperidine-1-oxyl radical) cellulose nanofibrils (TEMPO CNF) for the

immobilization of phototrophic microbes was investigated. To produce TEMPO CNF, cellulose fibrils (usually obtained from wood) are oxidized using TEMPO as a catalyst. In this oxidation process, the outermost hydroxyl groups of the cellulose fibers are oxidized to carboxylic groups. After this oxidation, the cellulose nanofibrils (3 – 4 nm wide and a few µm long) are mechanically disintegrated from the cellulose fibers (Saito et al., 2006). TEMPO CNF has several favorable features over the more widely used alginate immobilization matrix. The major benefit of cellulose nanofibrils over the alginate, is the porous fibrillar structure of the nanofibrils compared with alginate single polymer chains (Lee and Mooney, 2012; Mautner et al., 2014). For example, in our studies it enabled more efficient hydrogen production as discussed later.

In order to test the potential of TEMPO CNF for use in photohydrogen bioproduction, the biocompatibility and performance of TEMPO CNF was evaluated by entrapping phototropic microbes into the matrix and measuring hydrogen production. Three different approaches were used to immobilize the model filamentous cyanobacteria or green alga to the TEMPO CNF matrix: (i) TEMPO CNF hydrogel, (ii) Ca^{2+}-stabilized TEMPO CNF, (iii) the TEMPO CNF solid thin-films cross-linked with PVA.

4.7.1 Approach A: TEMPO CNF hydrogel

The biocompatibility of TEMPO CNF was tested by entrapping the Δ*hupL* mutant of *Anabaena* sp. PCC7120 cells inside the matrix, which was followed by a hydrogen photoproduction phase. During this hydrogen production phase, H_2 and O_2 yields were measured and the effective Photosystem II yield was measured at the beginning and end of production. As they are commonly used in other studies, Ca^{2+}-crosslinked alginate hydrogel entrapped cells were used as a reference. Besides this, matrix-free cells also served as a reference.

All of the samples yielded effectively the same amounts of hydrogen throughout the eight-day experiment (Paper III, Fig. 4A). The chlorophyll normalized maximum specific rates were statistically significantly higher ($P < 0.05$) for both TEMPO CNF and TEMPO CNF-PVA hydrogel samples compared with both of the reference samples. The maximum specific rates obtained are present in table 6.

Table 6. Maximum specific rates of H_2 production in the TEMPO CNF experiment.

Maximum specific rate	TEMPO CNF	TEMPO CNF-PVA	Alginate	Matrix-free cells
µmol H_2 * (mg chlorophyll*h)$^{-1}$	18.0	18.3	13.7	13.0
SD	0.7	0.9	1.3	0.3

Oxygen production, which was measured in parallel, also showed similar yields for all of the samples (Paper III, Fig. S1B). The biocompatibility of TEMPO CNF is highly supported by the aforementioned data, together with the effective Photosystem II yield (Paper III, Fig. S1A), which did not differ noticeably between the beginning and end of the experiment.

4.7.2 Approach B: TEMPO CNF hydrogel crosslinked with Ca^{2+}

To be able to develop submerged hydrogel layers, a sheet of insect screen was used as a support structure and a hydrogel layer added and stabilized with calcium. In this approach, a sulphur-deprived model green alga, *C. reinhardtii*, was used as the hydrogen producing strain.

In the hydrogel approach there was a clear difference in hydrogen photoproduction between TEMPO CNF-entrapped cells and alginate-entrapped cells. The TEMPO CNF-PVA-entrapped cells produced almost three times more hydrogen than the alginate-entrapped cells by the end of the experiment (Paper III, Fig. 4B). In addition, the effective Photosystem II yield (Y(II)) did not significantly differ between the samples (Paper III, Fig. S2). However, there was a significant drop of Y(II) in all of the samples from the start to the end of the experiment. This is explained by the sulphur-deprivation condition causing substantial stress to the cells.

4.7.3 Approach C: Solid cyanobacterial TEMPO CNF films

Calcium crosslinking itself is not enough to generate self-standing films with entrapped microbes. Thus, PVA-crosslinking was applied to *Anabaena* sp. PCC7120 Δ*hupL* mutant cells entrapped in TEMPO CNF hydrogel. The crosslinking was performed by drying the TEMPO CNF for 22 h in complete darkness at 23 °C and 70% relative humidity. After that, the cells were recovered for four days at 26 °C

under an air atmosphere supplemented with 0.5% CO_2, under 6 µmol photons m^{-2} s^{-1} PAR light intensity. The fitness of the cells was followed by measuring the effective Photosystem II yield (Y(II)) throughout these steps. The Y(II) value dropped significantly from values of over 0.45 to values lower than 0.25 during the drying step. This was presumably due to drought stress (Hirai et al., 2004).

After the recovery step, the films were placed in a similar hydrogen production setting as in approach A. In this case, alginate-entrapped cells showed the highest hydrogen production yields. However, the yields of TEMPO CNF -PVA films did not show substantially lower hydrogen yields compared with the alginate films. Particularly in the beginning of the nine-day experiment, the hydrogen production rates of matrix-free cells were considerably lower compared to both matrix-immobilization approaches. These results are encouraging for the continued development of self-standing films for the immobilization of phototrophic microbes inside the TEMPO CNF matrix.

4.7.4 Surface interaction studies with QCM-D

To investigate the possibility of passive attachment of microalgal cells to the surface of TEMPO CNF, surface interactions between Δ*hupL* mutant of *Anabaena* sp. PCC7120 and TEMPO CNF were studied using Quartz crystal microbalance with dissipation monitoring (QCM-D). First, the quartz crystal disc was coated with pure TEMPO CNF, but interactions were minimal, even after cells were dried on to the surface of the TEMPO CNF coating. Then it was decided to cationize the TEMPO CNF surface with polyethylenimine (PEI), as microalgal cells are known to have negative surface charge under neutral pH conditions (Lalonde et al., 2008). The addition of PEI had dramatic effects on interactions, with the attached cellular mass over an order of magnitude higher than on the untreated TEMPO CNF surface. As a next step, cationic nanocellulose, which does not require an additional coating step, could be utilized (Larsson et al., 2018).

5 DISCUSSION

5.1 Green alga UHCC0027 was the most efficient isolate for nutrient removal

Eight unicellular microalgae were selected from the University of Helsinki Culture Collection (UHCC) for nutrient removal and biomass accumulation. The green alga, UHCC0027, clearly stood out from the other isolates, especially in phosphate removal and biomass accumulation (Paper I, Fig.1). That an alga outperformed the cyanobacterial strains is not necessarily surprising, since hypereutrophicated waters are usually dominated by green algal species (Ma et al., 2015). Notably, the UHCC0027 cells performed better than the green algal control strain *Chlorella vulgaris*, a strain that is considered a good performer in wastewater treatment (Kainthola, 2016).

5.2 An increase in CO_2 concentration strongly enhanced nutrient removal

In order to test the isolates under more optimal conditions for efficient wastewater treatment, high light and high carbon tolerance were also screened. Again, under these conditions, the UHCC0027 cells showed the best performance of all strains. Cultures were supplied with 3% CO_2, which is commonly used for high carbon experiments, at least in algal physiology. It has been reported that the optimal CO_2 concentration for algae cultivation is somewhere between 5 to 10% (Tang et al. (2011), and some green algae species are able to grow even in the presence of 70% CO_2 in the gas phase (Singh and Singh, 2014). Carbon tolerance is important in different applications, e.g. flue gas CO_2 stripping, whereby a microalgae culture is supplied with flue gas (Kao et al., 2014).

As the optimized conditions again led to the UHCC0027 isolate performing the most efficient nutrient removal and biomass accumulation, a further study of the robustness of this strain was conducted using real wastewater. In this study, the effect

of high and low CO_2 concentration on growth in both synthetic and real wastewater was studied. This was done in experiments where an 18:6 hour light-dark cycle was applied, as it would allow energy savings in future applications (Bouterfas et al., 2006).

Results of the low carbon (ambient CO_2) experiment, performed in real municipal wastewater, were influenced by wastewater indigenous phototrophs. This influence was particularly noticeable in chlorophyll a and phosphate removal curves (Paper I, Fig. 3B&D). In both curves there are clear drops around day eight, caused by normalization to the blank experiment, where the growth of wastewater indigenous algae had become apparent around the same time. The growth of wastewater indigenous phototrophs is a common phenomenon in experiments performed in real municipal wastewaters where drainage waters are also collected (Lau et al., 1996; Singh and Das, 2014).

The addition of high (3%) CO_2 concentration had the most dramatic effects on cell growth and other measured parameters (Paper I, Fig. 1). For example, in just two days, almost all measured nutrients were removed from the experiments supplemented with 3% CO_2. Enhanced nutrient removal after CO_2 supplementation has been observed in many previous studies (Qi et al., 2017; Singh et al., 2014) and is caused when the culture shifts from carbon limitation to light limitation or inhibition.

In general, green algae perform better at high CO_2 concentrations compared with cyanobacteria (Liu et al., 2013; Wang et al., 2018). For example, in a study performed by Wang et al. (2018), they found that green algal *Scenedesmus* species dominated the microalgal community when the water samples were enriched with high CO_2 (10%). However, there are some cyanobacterial strains that are also able to tolerate high concentrations of CO_2 (Choix et al., 2017). Since UHCC0027 sits in the Scenedesmaceae family, the reported high CO_2 tolerance of *Scenedesmus* species presents a possibility future utilization of the UHCC0027 isolate in CO_2 stripping from fuel gases. The tolerance of extremely high CO_2 concentrations (> 20%) is hypothesized to link to three key acclimation mechanisms managing pH homeostasis of the cells: (i) the acclimation of the photosynthetic apparatus, the active transport of protons from the cytoplasm into the vacuoles and (ii) shutdown of the CO_2-concentrating mechanism (CCM) and (iii) adjustment of membrane fatty acid composition (Solovchenko and Khozin-Goldberg, 2013). When the high CO_2 tolerant microalgal cells face the extremely high CO_2 concentrations, they increase the PSI/II ratio in thylakoid membranes, to enhance the cyclic electron flow around the PSI to increase ATP generation (Solovchenko and Khozin-Goldberg, 2013).

When the cells shutdown the CCM, usually it means that, the expression of carbonic anhydrase is often strongly downregulated (Solovchenko and Khozin-Goldberg, 2013).

Interestingly, the nutrients from the real municipal wastewater experiment were removed in percentage terms almost as rapidly as from synthetic wastewater. What makes it interesting, is the fact that the ammonia and phosphate concentrations were almost double in real municipal wastewater (section 3.2). The difference in nutrient starting levels is also seen in OD and chlorophyll a curves (Paper I, Fig. 3A & B), as both of them reached significantly higher levels during the five-day experiments. There are several plausible reasons for this phenomenon of more efficient growth in real municipal wastewater. One of the reasons is the existence of wastewater indigenous heterotrophic bacteria that are living in wastewater. They have a mutualistic relationship with the microalgae cells providing shelter and beneficial compounds (Unnithan et al., 2014). Another reason may be the presence of organic compounds (COD ~ 600 mg L^{-1}) that the cells are able to utilize for mixotrophic growth (Jiang et al., 2011). The benefit of municipal wastewater was also seen in measured photosynthetic performance values (Paper I, Fig. 4). However, this more likely linked to nutrient availability than the indigenous bacteria or mixotrophic growth (Cecchin et al., 2018; Samori et al., 2014).

5.3 Green alga UHCC0027 demonstrated the highest biodiesel potential based on neutral lipid content

In most eukaryotic cells, excess energy is stored as triacylglycerols (TAGs) in lipid droplets (Martin and Parton, 2006). However, these organelles are more rarely found in prokaryotes (Walther and Farese, 2009) such as actinobacteria and cyanobacteria. For example, there has been a relatively recent description of TAG accumulation in lipid droplets observed in an N_2-fixing cyanobacteria (Peramuna and Summers, 2014). Lipid droplets mainly consist of neutral lipids, which are considered suitable for biodiesel (Chen et al., 2018). To determine the potential of the ten isolates, neutral lipid contents were analyzed by applying BODIPY dye, which was detected using flow cytometry.

Neutral lipid signals from both green algal isolates were significantly higher than from cyanobacterial isolates (Paper I, Fig. 5) and the UHCC0027 isolate had a slightly higher fluorescence than the reference strain *Chlorella vulgaris*. The higher neutral lipid content of the green algae was not unexpected, as cyanobacteria generally store most of their excess energy as glycogen rather than lipids (Aikawa et

al., 2014). The difference between green algae and cyanobacteria would have likely been even more pronounced if the cells were harvested from nutrient deplete conditions (G Breuer et al., 2013).

The 0TU37S4 isolate (Rajaniemi-Wacklin et al., 2006) had an EPS (Extracellular polymeric substance) layer covering the cells. This made the analysis more complicated with this isolate, as the BODIPY dye attached to the EPS layer yielding an unspecific signal. This problem was resolved by washing with PBS buffer. Nevertheless, from a biotechnological viewpoint, these EPS compounds may be of great interest for their possible therapeutic effects (Arad and Levy-Ontman, 2010; Bavington and Moss, 2016). In future, it would be fascinating to study the potential of this isolate for such applications.

5.4 Pilot-scale reactors seeded with UHCC0027 met EU directive requirements for urban wastewater treatment

In many cases, when processes are scaled up from laboratory to pilot-scale, and further to industrial scale, efficiencies decrease (Van Den Hende et al., 2014). The performance of the UHCC0027 isolate was therefore studied in real municipal wastewater in a pilot-scale photobioreactor (PBR). As described earlier (section 3.2), experiments were performed using two wastewater types (HC_LN and LC_HN) dependent on the characteristics of the wastewater at the time of filling the reactors. A further cold temperature experiment was conducted to evaluate performance in a Nordic climate, this wastewater composition was LC_HN (denoted LC_HN cold).

5.4.1 Growth of UHCC0027 cells in real wastewater

The first difference, related to algal growth, between the two wastewater types (HC_LN and LC_HN), was the slightly faster chlorophyll growth rate in HC_LN experiment compared with LC_HN experiment. Throughout the HC_LN experiment, average temperature was lower than in LC_HN experiment (Paper II, Fig. S2). According to Arrhenius equation, all the enzymatic reactions should accelerate together with increasing temperature (Morgan-kiss et al., 2006), that should favor faster growth in LC_HN experiment. Nevertheless, the faster growth rate can be explained by the higher COD concentration in the HC_LN experiment, enabling mixotrophic growth and altering the C:N ratio which was demonstrated to be so important for this alga at laboratory scale (Lynch et al. 2015). It is also possible that the temperature exceeded the optimal growth temperature of the UHCC0027 alga (Xin et al., 2011) which is a native isolate of Finland. Temperatures which are

over that required for optimal growth can inhibit growth through several routes, including the unfolding of proteins and alterations in membrane fluidity (Béchet et al., 2017).

From the fifth day of both of the experiments (HC_LN and LC_HN), there is a clear increase in dry weight concentration (Paper II, Fig. 1C), likely caused by the growth of microalgae. This growth is more evident when the dry weight is plotted against chlorophyll concentration (Paper II, Fig. 1D). Around the same time, both blank experiments had decreasing dry weight concentrations, substantiating the microalgal contributions to biomass increases in the seeded reactors. The most interesting phenomenon related to the microalgae growth occurred in the cold experiment. At around day ten, there was a significant increase in dry weight normalized to chlorophyll concentration in both blank and cold experiments (Paper II, Fig. 1B). Microscopy analysis (Paper II, Fig. S3) confirmed the presence of a consortium of wastewater indigenous phototrophic microbes. It is generally accepted that microalgae consortiums are more efficient than monocultures over many aspects of wastewater treatment, including nutrient removal rates, resistance to grazers and biomass accumulation (Chen et al., 2015). It is thus possible, that in UHCC0027 inoculated experiments, the aforementioned parameters could have been further improved by the additional inoculation of the reactors with a consortium of microalgae at the beginning of the experiments.

5.4.2 Nutrient removal

Requirements of the UWWTD for nutrient removal were met in the UHCC0027 seeded ambient and cold temperature experiments (LC_HN and LC_HN cold), whereas in the blank experiment requirements were not reached within the 14-day timeframe. In all experiments, ammoniacal nitrogen (NH_4^+-N) was the most abundant component of nitrogen and in the experimental set-up used, there are several processes which remove ammoniacal nitrogen from the reactors. The most important of these processes are: ammonium air stripping, algal uptake, nitrification and precipitation (Arogo et al., 1999; Hanhoun et al., 2011; Kainthola, 2016). The blank experiment was a good reference for determining the contribution of each of these processes in the ambient temperature experiment. The pH of sampled wastewater was in a range where air stripping occurs (pH>8, Guštin and Marinšek-Logar, 2011). At the beginning of the experiments (days 0 to 2), the total dissolved nitrogen, nitrate and nitrite curves were almost identical in both experiments (Paper II, fig. S4), thus air stripping or precipitation were the most significant processes to remove ammoniacal nitrogen at that time. After this, a significant increase in nitrite and nitrate concentrations and decrease in pH occured in both the seeded and blank

experiments, demonstrating nitrification processes (Paper II, Fig. 2B). The decreasing pH is observed as nitrifying bacteria produce protons when growing (Sharma and Ahlert, 1977). This pH trend was subsequently reversed in the seeded reactor well before the blank reactor, implying a later role for microalgal uptake. Compared to the LC_HN experiments, maximum nitrification rates occured slightly later in both HC_LN experiments, likely caused by lower ammoniacal nitrogen concentrations, or the original number of nitrifying bacteria. By comparing the dissolved inorganic nitrogen (DIN) values in the beginning and at the end of the experiments, it was possible to conclude that the nitrification process was the most important in ammonical nitrogen removal.

In the cold experiment, the lack of blank control experiment made it difficult to evaluate the contribution of different ammoniacal nitrogen removal processes. In spite of this, it is known that the rates of air stripping and nitrification would be significantly lower at the temperatures employed in the cold experiment (Arogo et al., 1999; Saad and Conrad, 1993). This likely resulted in the similar profiles of the ammonical nitrogen and total dissolved nitrogen curves (Paper II, Fig 2C & D). However, the contribution of the wastewater indigenous phototrophic microbe consortium was able to be seen in nitrogen removal, whereby the maximum total dissolved nitrogen removal rates were almost equal at the exponential growth phase of ambient and cold temperature experiments.

Phosphorous removal is a particularly important aspect of wastewater treatment, especially in places where effluent water is released to inland waters or seas. The Baltic Sea is one example of a heavily eutrophicated sea where phosphorous discharge from agriculture is often responsible for cyanobacterial blooms (Ulrich et al., 2009). As in the earlier laboratory study (Lynch et al. 2015), the UHCC0027 strain demonstrated efficient phosphorous removal. Indeed, seeding of the strain was necessary for treatment to meet UWWTD requirements, with neither of the blank reactors reaching final phosphate levels lower than initial levels. Another interesting observation was the faster maximum rate of phosphate removal in the cold experiment. This occurred over days 18 to 20, when the wastewater indigenous phototrophic microbes were active. The higher N:P ratio in the cold reactor, which had much lower rates of nitrogen removal throughout the experiment, was likely responsible for this high phosphorous removal performance (Beuckels et al., 2015).

A tiny peak in the phosphorous curves of the cold experiment was observed late in the experiment, around the same time grazers were observed consuming phototrophic cells (Paper II, S3). This demonstrates the importance of predator management, as has been discussed for large scale cultivation (Montemezzani et al., 2015).

5.5 Wastewater grown UHCC0027 cells showed typical FAME profiles and biodiesel properties for microalgal cells

It is a highly attractive option to integrate microalgal wastewater treatment with biodiesel production, as the process is very synergistic. The study of wastewater grown microalgae biodiesel potential was included for this reason. Samples were taken for analysis at three different points of the experiments (pre-growth, middle growth and late exponential growth phase).

To estimate the quantities of obtainable biodiesel, total-lipid contents were measured gravimetrically. The most distinctive observation from the measurements was the clear increase in the lipid content in the ambient temperature culture at the late exponential growth phase (Paper II, Fig. 2A). Nitrogen starvation is usually responsible for such an increase (Xin et al., 2010). Whilst cells were not nitrogen starved, available nitrogen was considerably lower after only four days at room temperature. The cold temperature experiment did not show a nitrogen depletion effect, lipid contents were approximately equal at the middle and late exponential growth phases. However, an increase was already seen from the pre-culture cold grown cells to the mid growth phase cells. This may be explained by the combined effects of cold temperature, known to increase lipid content, and wastewater, known as a stressful environment for microalgal cells (Guido Breuer et al., 2013; Osundeko et al., 2014), experienced after the transfer from synthetic wastewater to real wastewater.

To be able to predict the specific biodiesel properties obtained after transesterification, a detailed FAME analysis was performed. The samples were taken at the same time points as in the total-lipid analysis. The obtained FAME profiles (Paper II, Fig. 4B & C) were representative of typical green algae profiles (Schwenk et al., 2013) and in cold temperatures the unsaturated fatty acids were more abundant than at ambient temperature, which is unfavorable from a biodiesel point of view (Islam et al., 2013). The most abundant fatty acids (palmitate (C16:0) and α-linolenate (C18:3)) have opposing effects on the quality of the obtained biodiesel, as palmitate is highly desirable and α-linolenate is undesirable (Ramos et

al., 2009). In general, the unsaturated fatty acids tend to lower the cetane number and oxidation stability (Gopinath et al., 2010). For these reasons, the maximum percentage of linolenate is limited to 12% in European biodiesel standard EN 14214 (Melero et al., 2010).

None of the biodiesel properties, predicted based on the FAME profiles, met the requirements of USA standard ASTM D6751–02 nor European standard EN 14214 set for biodiesel. Nonetheless, this problem can be avoided by several means. Perhaps the simplest solution is to blend the obtained biodiesel with higher quality diesel or add some chemical additives to improve the properties. Another possibility is to follow the general trend in the bio-based diesel market, which is shifting towards the entry of hydrogenated vegetable oils (Wilde and Londo, 2009). In this process, the fatty acids are hydrogenated into long alkanes, after which the unsaturation degree does not play any role in the diesel properties (Liu et al., 2011).

5.6 Immobilization using cellulose nanofibrils increases the hydrogen yield of *Chlamydomonas reinhardtii*

Whilst the efficiency of biodiesel production was approached via integration with waste processes and low energy production techniques, the approach employed for photobiological H_2 production was to improve the efficiency of light utilization via immobilization using a novel material. Currently, alginate is the most used matrix for the immobilization of phototrophic microbes. However, it has some disadvantages including low porosity and mechanical stability (Jämsä et al., 2018) and is well known to readily degrade in real wastewater (Cruz et al., 2013). Indeed, the attempted use of alginate beads in the afore described wastewater pilot-scale studies failed due to the degradation of the beads during preliminary experiments (data not published).

Following the failure of alginate to remain stable in real wastewater, TEMPO-oxidized cellulose nanofibrils (TEMPO CNF) were hypothesized to provide a superior immobilization alternative. This is due to the β(1→4) linked D-glucose units in the cellulose chain, which are known to be very stable due to the hydrogen bonding between hydroxyl groups. These links are found in the first and fourth positions of the carbon ring, between glucose units. Since the catalytic activities of cellulases could be considered to be an order of magnitude slower than alginate degrading enzymes, it was anticipated that bacterial degradation in wastewater would be significantly slower (Hakalahti et al., 2015; Li et al., 2018; Rajan and

Carrier, 2014). However, this hypothesis would need to be validated in experiments performed with real wastewater Along with mechanical strength, the highly controllable pore size of TEMPO CNF was anticipated to be a significant advantage in biofuel production. Particularly hydrogen production, where oxidative stress induced by the O_2 produced during photosynthesis has been shown to inhibit hydrogen production (Kosourov et al. 2017). Thus, it was decided to test the biocompatibility of TEMPO CNF for hydrogen production. Initial studies were performed using the well studied hydrogen producing cyanobacteria, *Anabaena sp.* Δ*hupL*. Cells were entrapped inside the TEMPO CNF hydrogel to study the biocompatibility and an additional evaluation of TEMPO CNF was undertaken with PVA added to form a film which was cross-linked by drying. Based on the measured photosynthetic activity and hydrogen yield, both TEMPO CNF and TEMPO CNF with PVA were fully biocompatible with *Anabaena* sp. Δ*hupL* cells. Since *Anabaena* cells are known to be quite tolerant of environmental stress (Pandey et al., 2012), this encouraged continuing with *C. reinhardtii* cells.

The maximum specific rates of cyanobacterial hydrogen production shown in table 6 are comparable with the study performed by Leino et al. (2012). In that study, they obtained the maximum specific rates of 30 μmol H_2*(mg chlorophyll*h)$^{-1}$ for the alginate immobilized *Anabaena* sp. Δ*hupL* cells, whereas in this study the maximum rate was 14 μmol H_2*(mg chlorophyll*h)$^{-1}$. However, the results are not directly comparable, as the aerial chlorophyll concentration was approximately three times higher in this study. This may result in oxygen inhibition of hydrogen production due to higher cell density. As the maximum rate in this study was 18 H_2*(mg chlorophyll*h)$^{-1}$ for TEMPO CNF immobilized Δ*hupL* cells, it could be linearly extrapolated that with less dense films the maximum rates could reach at least over 38 H_2*(mg chlorophyll*h)$^{-1}$.

The experiment performed with *C. reinhardtii* cells required a more mechanically stable matrix. To achieve this, insect screen was used as a support for the hydrogel layers and the matrix was calcium cross-linked. Here, the TEMPO-CNF and TEMPO-CNF with PVA showed significantly higher hydrogen yields than alginate layers. This was most likely caused by the differences in the entrapping material, as the TEMPO CNF has a unique fibrillary structure compared with alginate (Paper III, Fig. 5). These fibers presumably make the material more porous, allowing more efficient gas exchange with the surrounding gas phase. The hydrogen production rates with *C. reinhardtii* cells are known to decline when hydrogen partial pressure increases and likely inhibits production rates inside the alginate matrix (Kosourov et al., 2012).

To be able to make self-standing films from TEMPO-CNF, a suitable cross-linking method was needed. Due to previous experience cross-linking using PVA, it was chosen as a suitable polymer (Hakalahti et al., 2015). The cross-linking was performed by drying films so that ester bonds are formed between the hydroxyl groups of PVA and carboxylic groups of TEMPO-CNF.
The fitness of the cells was followed throughout the drying and subsequent recovery step. According to the effective photosystem II yield and the observed hydrogen yields, the cells recovered well (Paper III. Fig. 5A to C). Only the control cells (without any matrix) suffered significantly from the drying step.

A noticeable difference was observed in the masses of the corresponding matrix around the cells. In the alginate films, it was calculated that there was at least four times more matrix around the cells than that used in TEMPO-CNF samples. It is very likely that the matrix protected the cells during drying, with differently treated cells thus experiencing different drought stress levels. This hypothesis was supported by an additional experiment (data not published), where masses of TEMPO-CNF and alginate around the cells were equalized and subsequent photosystem II yields and hydrogen yields of TEMPO-CNF and alginate samples were equalized.

6 CONCLUSIONS AND FUTURE PERSPECTIVES

In this Ph.D. project, I have endeavored to improve the efficiencies of photoautotrophic biofuel production by investigating two promising strategies: (i) Integrative biomass-based production: screening native Finnish microalgae for integrated wastewater treatment and biodiesel production, optimizing process conditions, and scaling up and performing detailed analysis of biodiesel potential; (ii) Direct biofuel/chemical production: immobilization of green algae and cyanobacteria in nanocellulose material for optimized efficiency of biofuel production through the restriction of biomass accumulation and re-direction of energy to targeted products, so that the photosynthetic microbes act as true biocatalysts.

The key findings of this thesis were:

- A native alga, UHCC00027 of the Scenedesmaceae family, was the most efficient strain in nutrient removal, biomass and lipid accumulation and wasable to fulfil the EU UWWTD for phosphorus removal under low energy conditions at laboratory scale

- Carbon nitrogen balance played an important role in biomass accumulation and nutrient removal performance. Enhanced performance was achieved through the manipulation of this balance

- Pilot-scale reactors, seeded with UHCC0027, were able to fulfil the EU directive requirements for urban wastewater treatment

- In pilot scale studies, under cold temperatures, nitrogen phosphorous balance and the growth of wastewater indigenous phototrophic organisms were important in phosphorous removal performance

- Manipulation of the growth conditions could be manipulated to achieve very good N&P removal at Nordic conditions whilst producing high quantities of lipids

- The lipid profile of algal biomass obtained from real wastewater at pilot scale, and hence biodiesel quality, were impacted by the temperature of algal growth.

- TEMPO oxidized cellulose nanofibrils (TEMPO CNF) are biocompatible with cyanobacterial and green algal cells

- *Chlamydomonas reinhardtii* cells entrapped in TEMPO CNF demonstrated substantially higher hydrogen yields compared to alginate entrapped cells

- Entrapped Δ*hupL* mutant cells of *Anabaena* sp. PCC7120 could recover and produce hydrogen after drying, which was required for stable film formation

These key findings have presented opportunities for further studies. For example, it would be interesting to isolate and learn more about the phototrophic consortium that was established in real wastewater under cold conditions. The stability and performance of this consortium could be evaluated against other consortiums, which may be naturally occurring, or man-made. The finding that TEMPO CNF is biocompatible with microalgal cells is particularly promising, allowing the evaluation of this immobilization material in real wastewater, where the use of alginate can be limited due to degradation. The higher porosity of TEMPO CNF compared to other entrapment matrices may even enable the entrapment of microalgae which are genetically modified to produce and release molecules larger than hydrogen.

Overall, the work presented in this PhD thesis demonstrates potential for the industrial application of microalgae under Nordic conditions. By demonstrating improved efficiencies of the relevant processes, the findings presented here may facilitate the implementation of wastewater and biofuel applications as they become increasingly attractive to both the public and private sector. However, feasibility will need to be demonstrated under conventional operational conditions (i.e. year round, continuous or semi-continous modes) before a shift to full scale production would be expected. Nevertheless, it is anticipated that the research presented, particularly in regard to improving efficiencies of biofuel production, will also translate to other regions and situations currently considered unfavorable for microalgae cultivation. This study, together with other research efforts in the microalgae field, will expedite the shift towards more sustainable, large scale microalgal energy production.

7 ACKNOWLEDGEMENTS

This work was performed at the Laboratory of Molecular Plant Biology at the University of Turku. Financial support from the Academy of Finland Center of Excellence Project, Nordic Centre of Excellence (NCoE, NordAqua) funded by NordForsk, Novo Nordisk Foundation and Kone foundation is gratefully acknowledged.

I warmly thank my supervisor Assoc. Prof. Yagut Allahverdiyeva-Rinne and Academician Eva-Mari Aro for giving me a change to work in one of the leading laboratories in the field of photosynthesis in world. In addition, I acknowledge my supervisor Dr. Fiona Lynch for the practical guidance and language revision both the thesis and manuscripts. Dr. Sergey Kosourov is warmly thanked for the practical guidance during the nanocellulose project and all the refreshing discussions about everything under the sun. Besides, I would like to express my gratitude to Prof. Eevi Rintamäki for the guidance throughout the Ph.D. studies and especially at the bureaucratic steps of the graduation.

All my co-authors are thanked for their contribution and support. Especially, I would like to acknowledge Dr. Jukka Ketoja and Dr. Tekla Tammelin from VTT for believing in the idea of nanocellulose immobilization. In addition, Ville Rissanen and Dr. Minna Hakalahti are thanked for the common brainstorming and sharing of practical knowledge. Besides, Petteri Laaksonen from Clewer Ltd. is highly acknowledged for the practical guidance during the wastewater studies.

I would like to thank all my colleagues and fellows at the laboratory for the nice moments. Especially, I would like to express my gratitude to Dr. Mika Keränen for the help with practical issues and the pleasant chats, mainly related to politics.
Finally, I am truly grateful to my family and friends. Kiitos, Äiti, Isä (muistoissani), Henrik, Maiju, Tuulia, Jukka, Ritva, Henri, Maarit, Nooa, Camilla, Heidi, Hanna, Onni, Lilja, Merja, Pihla, Meri, Tuukka, Sara ja Leena. Erityisesti haluaisin kiittää Lassia ja Tanelia kaikista tieteen ympärillä käydyistä lukuisista keskusteluista.

Suurimmat kiitokset ansaitsee Tuulikki kaikesta tuesta ja ymmärryksestä, tiedät mitä se on vaatinut! Lisäksi suurimmat kiitokseni menee pojalleni Oliverille, joka on aina jaksanut päivästä toiseen piristää jutuillaan.

List of references

Aikawa, S., Nishida, A., Ho, S.H., Chang, J.S., Hasunuma, T., Kondo, A., (2014). Glycogen production for biofuels by the euryhaline cyanobacteria *Synechococcus* sp. strain PCC 7002 from an oceanic environment. Biotechnol. Biofuels **7**: 1–8. doi:10.1186/1754-6834-7-88

Ajjawi, I., Verruto, J., Aqui, M., Soriaga, L.B., Coppersmith, J., Kwok, K., Peach, L., Orchard, E., Kalb, R., Xu, W., Carlson, T.J., Francis, K., Konigsfeld, K., Bartalis, J., Schultz, A., Lambert, W., Schwartz, A.S., Brown, R., Moellering, E.R., (2017). Lipid production in *Nannochloropsis* gaditana is doubled by decreasing expression of a single transcriptional regulator. Nat. Biotechnol. **35**: 647–652. doi:10.1038/nbt.3865

Allahverdiyeva, Y., Aro, E.M., Kosourov, S.N., (2014). Recent Developments on Cyanobacteria and Green Algae for Biohydrogen Photoproduction and Its Importance in CO_2 Reduction, in: Bioenergy Research: Advances and Applications. Elsevier, pp. 367–387. doi:10.1016/B978-0-444-59561-4.00021-8

Arad, S., Levy-Ontman, O., (2010). Red microalgal cell-wall polysaccharides: Biotechnological aspects. Curr. Opin. Biotechnol. **21**: 358–364. doi:10.1016/j.copbio.2010.02.008

Aro, E.M., (2016). From first generation biofuels to advanced solar biofuels. Ambio **45:** 24–31. doi:10.1007/s13280-015-0730-0

Arogo, J., Zhang, R.H., Riskowski, G.L., Christianson, L.L., Day, D.L., (1999). Mass Transfer Coefficient of Ammonia in Liquid Swine Manure and Aqueous Solutions. J. Agric. Eng. Res. **73**: 77–86. doi:10.1006/jaer.1998.0390

Barsanti, L., Gualtieri, P., (2014). Algae: anatomy, biochemistry, and biotechnology. CRC press. p.1–139

Bavington, C.D., Moss, C., (2016). Polysaccharides from prasinococcales. United States Patent US 9.453,082 B2 Sep. 27, 2016

Béchet, Q., Laviale, M., Arsapin, N., Bonnefond, H., Bernard, O., (2017). Modeling the impact of high temperatures on microalgal viability and photosynthetic activity. Biotechnol. Biofuels **10**: 1–11. doi:10.1186/s13068-017-0823-z

Bekker, A., Holland, H.D., Wang, P.L., Rumble, D., Stein, H.J., Hannah, J.L., Coetzee, L.L., Beukes, N.J., (2004). Dating the rise of atmospheric oxygen. Nature **427**: 117–120. doi:10.1038/nature02260

Beuckels, A., Smolders, E., Muylaert, K., (2015). Nitrogen availability influences phosphorus removal in microalgae-based wastewater treatment. Water Res. **77:** 98–106. doi:10.1016/j.watres.2015.03.018

Bouterfas, R., Belkoura, M., Dauta, A., (2006). The effects of irradiance and photoperiod on the growth rate of three freshwater green algae isolated from a eutrophic lake Source of the organisms isolated from the eutrophic Takerkoust barrage ' s. Lemnetica **25:** 647–656. doi:10.1023/A:1023241006464

Breuer, G., Lamers, P.P., Martens, D.E., Draaisma, R.B., Wijffels, R.H., (2013). Effect of light intensity, pH, and temperature on triacylglycerol (TAG) accumulation induced by nitrogen starvation in *Scenedesmus obliquus*. Bioresour. Technol. **143:** doi:10.1016/j.biortech.2013.05.105

Carney, L.T., Lane, T.W., (2014). Parasites in algae mass culture. Front. Microbiol. **5:** 1–8. doi:10.3389/fmicb.2014.00278

Cecchin, M., Benfatto, S., Griggio, F., Mori, A., Cazzaniga, S., Vitulo, N., Delledonne, M., Ballottari, M., (2018). Molecular basis of autotrophic vs mixotrophic growth in *Chlorella sorokiniana.* Sci. Rep. **8:** 1–13. doi:10.1038/s41598-018-24979-8

Chandrasekhar, K., Lee, Y.-J., Lee, D.-W., (2015). Biohydrogen Production: Strategies to Improve Process Efficiency through Microbial Routes. Int. J. Mol. Sci. **16:** 8266–8293. doi:10.3390/ijms16048266

Chen, G., Zhao, L., Qi, Y., (2015). Enhancing the productivity of microalgae cultivated in wastewater toward biofuel production: A critical review. Appl. Energy **137:** 282–291. doi:10.1016/j.apenergy.2014.10.032

Chen, Z., Wang, L., Qiu, S., Ge, S., (2018). Determination of Microalgal Lipid Content and Fatty Acid for Biofuel Production. Biomed Res. Int. **1503126:** pp.1-17. doi:10.1155/2018/1503126

Chochois, V., Dauvillee, D., Beyly, A., Tolleter, D., Cuine, S., Timpano, H., Ball, S., Cournac, L., Peltier, G., (2009). Hydrogen Production in Chlamydomonas: Photosystem II-Dependent and -Independent Pathways Differ in Their Requirement for Starch Metabolism. Plant Physiol. **151:** 631–640. doi:10.1104/pp.109.144576

Choix, F.J., Snell-Castro, R., Arreola-Vargas, J., Carbajal-López, A., Méndez-Acosta, H.O., (2017). CO_2 Removal from Biogas by Cyanobacterium *Leptolyngbya* sp. CChF1 Isolated from the Lake Chapala, Mexico: Optimization of the Temperature and Light Intensity. Appl. Biochem. Biotechnol. **183:** 1304–1322. doi:10.1007/s12010-017-2499-z

Collos, Y., Harrison, P.J., (2014). Acclimation and toxicity of high ammonium concentrations to unicellular algae. Mar. Pollut. Bull. **80:** 8–23. doi:10.1016/j.marpolbul.2014.01.006

Cordell, D., White, S., (2011). Peak phosphorus: Clarifying the key issues of a vigorous debate about long-term phosphorus security. Sustainability **3:** 2027–2049. doi:10.3390/su3102027

Corley, C.E., (2011). Principles of design and operations of wastewater treatment pond systems for plant operators, engineers, and managers. Illinois Environ. Prot. Agency **600:** 1–457.

Craggs, R.J., Sutherland, D., Campbell, H., (2010). World-first wastewater algal bio- crude oil demonstration.

Cruz, I., Bashan, Y., Hernàndez-Carmona, G., De-Bashan, L.E., (2013). Biological deterioration of alginate beads containing immobilized microalgae and bacteria during tertiary wastewater treatment. Appl. Microbiol. Biotechnol. **97:** 9847–9858. doi:10.1007/s00253-013-4703-6

Dahiya, A., Krivov, A., Dahiya, A., 2014. Biomass to Biofuels : Biomass to Biofuels. Elsevier Science & Technology, San Diego, US.

de-Bashan, L.E., Bashan, Y., (2010). Immobilized microalgae for removing pollutants: Review of practical aspects. Bioresour. Technol. **101:** 1611–1627. doi:10.1016/j.biortech.2009.09.043

Dekker, J.P., Boekema, E.J., (2005). Supramolecular organization of thylakoid membrane proteins in green plants. Biochim. Biophys. Acta - Bioenerg. **1706:** 12–39. doi:10.1016/j.bbabio.2004.09.009

Delrue, F., Álvarez-Díaz, P., Fon-Sing, S., Fleury, G., Sassi, J.-F., (2016). The Environmental Biorefinery: Using Microalgae to Remediate Wastewater, a Win-Win Paradigm. Energies **9:** 132. doi:10.3390/en9030132

Devle, H., Rukke, E.O., Naess-Andresen, C.F., Ekeberg, D., (2009). A GC - Magnetic sector MS method for identification and quantification of fatty acids in ewe milk by different acquisition modes. J. Sep. Sci. **32:** 3738–3745. doi:10.1002/jssc.200900455

Domozych, D.S., Ciancia, M., Fangel, J.U., Mikkelsen, M.D., Ulvskov, P., Willats, W.G.T., (2012). The Cell Walls of Green Algae: A Journey through Evolution and Diversity. Front. Plant Sci. **3:** 1–7. doi:10.3389/fpls.2012.00082

Drath, M., Kloft, N., Batschauer, A., Marin, K., Novak, J., Forchhammer, K., (2008). Ammonia Triggers Photodamage of Photosystem II in the Cyanobacterium *Synechocystis* sp. Strain PCC 6803. Plant Physiol. **147:** 206–215. doi:10.1104/pp.108.117218

Ebenhöh, O., Spelberg, S., (2018). The importance of the photosynthetic Gibbs effect in the elucidation of the Calvin-Benson-Bassham Cycle. Biochem Soc Trans. **46:** 131–140. doi:10.1101/200105

Eroglu, E., Melis, A., (2016). Microalgal hydrogen production research. Int. J. Hydrogen Energy **41:** 12772–12798. doi:10.1016/j.ijhydene.2016.05.115

Field, C.B., Behrenfeld, M.J., Randerson, J.T., Falkowski, P., Field, C.B., Behrenfeld, M.J., Randerson, J.T., (1998). Primary Production of the Biosphere : Integrating Terrestrial and Oceanic Components **281:** 237–240.

Fleming, J.R., (2005). Historical Perspectives on Climate Change. New York: Oxford Univ. Press

Flores, E., Herrero, A., (2005). Nitrogen assimilation and nitrogen control in cyanobacteria. Biochem. Soc. Trans. **33:** 164 LP-167.

Gasol, J.M., Del Giorgio, P.A., Duarte, C.M., (1997). Biomass distribution in marine planktonic communities. Limnol. Oceanogr. **42:** 1353–1363. doi:10.4319/lo.1997.42.6.1353

Ghirardi, M.L., Dubini, A., Yu, J., Maness, P.C., (2009). Photobiological hydrogen-producing systems. Chem. Soc. Rev. **38:** 52–61. doi:10.1039/b718939g

Golbeck, J.H., (2006). Photosystem I : the light-driven plastocyanin : ferredoxin oxidoreductase. Springer, Dordrecht, The Netherlands

Gopinath, A., Puhan, S., Nagarajan, G., (2010). Effect of unsaturated fatty acid esters of biodiesel fuels on combustion, performance and emission characteristics of a DI diesel engine. Int. J. Energy Environ. **1:** 411-430

Guštin, S., Marinšek-Logar, R., (2011). Effect of pH, temperature and air flow rate on the continuous ammonia stripping of the anaerobic digestion effluent. Process Saf. Environ. Prot. **89:** 61–66. doi:10.1016/j.psep.2010.11.001

Hakalahti, M., Salminen, A., Seppälä, J., Tammelin, T., Hänninen, T., (2015). Effect of interfibrillar PVA bridging on water stability and mechanical properties of TEMPO/$NaClO_2$ oxidized cellulosic nanofibril films. Carbohydr. Polym. **126:** 78–82. doi:10.1016/j.carbpol.2015.03.007

Hanhoun, M., Montastruc, L., Azzaro-Pantel, C., Biscans, B., Frèche, M., Pibouleau, L., (2011). Temperature impact assessment on struvite solubility product: A thermodynamic modeling approach. Chem. Eng. J. **167:** 50–58. doi:10.1016/j.cej.2010.12.001

Hansen, J., Ruedy, R., Sato, M., Lo, K., (2010). Global surface temperature change. Rev. Geophys. **48:** RG4004. doi:10.1029/2010RG000345

Harris, E.H., (1989). The Chlamydomonas sourcebook: a comprehensive guide to biology and laboratory use. Academic Press, San Diego.

Henry, J.T., Crosson, S., (2013). Chromosome replication and segregation govern the biogenesis and inheritance of inorganic polyphosphate granules. Mol. Biol. Cell **24:** 3177–3186. doi:10.1091/mbc.E13-04-0182

Ho, L.T., Van Echelpoel, W., Goethals, P.L.M., (2017). Design of waste stabilization pond systems: A review. Water Res. **123:** 236–248. doi:10.1016/j.watres.2017.06.071

Hoekman, S.K., Broch, A., Robbins, C., Ceniceros, E., Natarajan, M., (2012). Review of biodiesel composition, properties, and specifications. Renew. Sustain. Energy Rev. **16:** 143–169. doi:10.1016/j.rser.2011.07.143

Hoiczyk, E., Hansel, A., (2000). Cyanobacterial cell walls: News from an unusual prokaryotic envelope. J. Bacteriol. **182:** 1191–1199. doi:10.1128/JB.182.5.1191-1199.2000

Houghton, R.A., (2007). Balancing the Global Carbon Budget. Annu. Rev. Earth Planet. Sci. **35:** 313–347. doi:10.1146/annurev.earth.35.031306.140057

Idriss, H., Scott, M., Subramani, V., (2015). Introduction to hydrogen and its properties, in: Compendium of Hydrogen Energy. pp. 3–19. Woodhead Publishing, Sawston, Cambridge, UK, doi:10.1016/B978-1-78242-361-4.00001-7

Islam, M.A., Magnusson, M., Brown, R.J., Ayoko, G.A., Nabi, M.N., Heimann, K., (2013). Microalgal species selection for biodiesel production based on fuel properties derived from fatty acid profiles. Energies **6:** 5676–5702. doi:10.3390/en6115676

Jämsä, M., Kosourov, S., Rissanen, V., Hakalahti, M., Pere, J., Ketoja, J.A., Tammelin, T., Allahverdiyeva, Y., (2018). Versatile templates from cellulose nanofibrils for photosynthetic microbial biofuel production. J. Mater. Chem. A **6:** 5825–5835. doi:10.1039/C7TA11164A

Janssen, G.J., Roy, E., Matysik, J., Alia, A., (2012). 15N Photo-CIDNP MAS NMR To Reveal Functional Heterogeneity in Electron Donor of Different Plant Organisms. Appl. Magn. Reson. **42:** 57–67. doi:10.1007/s00723-011-0283-8

Jiang, L., Luo, S., Fan, X., Yang, Z., Guo, R., (2011). Biomass and lipid production of marine microalgae using municipal wastewater and high concentration of CO_2. Appl. Energy **88:** 3336–3341. doi:10.1016/j.apenergy.2011.03.043

Joy, J., Mathew, J., George, S.C., (2018). Nanomaterials for photoelectrochemical water splitting – review. Int. J. Hydrogen Energy **43:** 4804–4817. doi:10.1016/j.ijhydene.2018.01.099

Kainthola, J., (2016). Tertiary Treatment of Wastewater with *Chlorella Vulgaris*- A Literature Review. J. Environ. Sci. Toxicol. Food Technol. **10:** 33–39. doi:10.9790/2402-1003023339

Kanatt, S.R., Tari, S., Chawla, S.P., (2018). Encapsulation of extract prepared from irradiated onion scales in alginate beads: a potential functional food ingredient. J. Food Meas. Charact. **12:** 848–858. doi:10.1007/s11694-017-9699-7

Kao, C.Y., Chen, T.Y., Chang, Y. Bin, Chiu, T.W., Lin, H.Y., Chen, C. Da, Chang, J.S., Lin, C.S., (2014). Utilization of carbon dioxide in industrial flue gases for the cultivation of microalga *Chlorella* sp. Bioresour. Technol. **166:** 485–493. doi:10.1016/j.biortech.2014.05.094

Karatzos, S., Mcmillan, J., Saddler, J., (2014). The potential and challenges of drop in biofuels, IEA Bioenergy Task. doi:10.1016/S0734-743X(96)00032-2 ISBN: 978-1-910154-07-6

Kessler, E., Huss, V.A.R., (1992). Comparative physiology and biochemistry and taxonomic assignment of the *Chlorella* (Chlorophyceae) strains of the culture collection of the University of Texas at Austin. J. Phycol. **28:** 550–553. doi:10.1111/j.0022-3646.1992.00550.x

Khanna, N., Lindblad, P., (2015). Cyanobacterial hydrogenases and hydrogen metabolism revisited: Recent progress and future prospects. Int. J. Mol. Sci. **16:** 10537–10561. doi:10.3390/ijms160510537

Kirilovsky, D., (2015). Modulating energy arriving at photochemical reaction centers: Orange carotenoid protein-related photoprotection and state transitions. Photosynth. Res. **126:** 3–17. doi:10.1007/s11120-014-0031-7

Knothe, G., Van Gerpen, J.H., Krahl, J.J., Gerpen, J.H. Van, (2005). The Biodiesel Handbook, Applied Sciences. AOCS Publishing, New York, US, doi:10.1201/9781439822357

Komarek, J., (2006). Cyanobacterial Taxonomy: Current Problems and Prospects for the Integration of Traditional and Molecular Approaches. Algae **21:** 349–375.

Kosourov, S., Jokel, M., Aro, E.-M., Allahverdiyeva, Y., (2018 A). A new approach for sustained and efficient H_2 photoproduction by *Chlamydomonas reinhardtii*. Energy Environ. Sci. **11:** 1431–1436. doi: 10.1039/c8ee00054a

Kosourov, S., Murukesan, G., Seibert, M., Allahverdiyeva, Y., (2017). Evaluation of light energy to H_2 energy conversion efficiency in thin films of cyanobacteria and green alga under photoautotrophic conditions. Algal Res. **28:** 253–263. doi:10.1016/j.algal.2017.09.027

Kosourov, S.N., Batyrova, K.A., Petushkova, E.P., Tsygankov, A.A., Ghirardi, M.L., Seibert, M., (2012). Maximizing the hydrogen photoproduction yields in *Chlamydomonas reinhardtii* cultures: The effect of the H_2 partial pressure. Int. J. Hydrogen Energy **37:** 8850–8858. doi:10.1016/j.ijhydene.2012.01.082

Kosourov, S.N., He, M., Allahverdiyeva, Y., Seibert, M., (2018 B). Chapter 15: Immobilization of Microalgae as a Tool for Efficient Light Utilization in H_2 Production and Other Biotechnology Applications, in: Microalgal Hydrogen Production: Achievements and Perspectives. The Royal Society of Chemistry, Croydon, UK, pp. 355–384. doi:10.1039/9781849737128-00355

Kosourov, S.N., Seibert, M., (2009). Hydrogen photoproduction by nutrient-deprived *Chlamydomonas reinhardtii* cells immobilized within thin alginate films under aerobic and anaerobic conditions. Biotechnol. Bioeng. **102:** 50–58. doi:10.1002/bit.22050

Kotai, J., (1972). Instructions for preparation of modified, nutrient solution Z8 for algae. Publication B-11/69. Norwegian Institute for Water Research, Oslo.

Lal, R., (2008). Carbon sequestration. Philos. Trans. R. Soc. B Biol. Sci. **363:** 815–830. doi:10.1098/rstb.2007.2185

Lalonde, S. V., Smith, D.S., Owttrim, G.W., Konhauser, K.O., (2008). Acid-base properties of cyanobacterial surfaces. II: Silica as a chemical stressor influencing cell surface reactivity. Geochim. Cosmochim. Acta **72:** 1269–1280. doi:10.1016/j.gca.2007.10.032

Lampert, W., Rothhaupt, K.O., von Elert, E., (1994). Chemical induction of colony formation in a green alga (*Scenedesmus acutus*) by grazers (*Daphnia*). Limnol. Oceanogr. **39:** 1543–1550. doi:10.4319/lo.1994.39.7.1543

Larsson, P.T., Hellwig, J., López Durán, V., Larsson, P.A., Wågberg, L., (2018). Effect of Chemical Functionality on the Mechanical and Barrier Performance of Nanocellulose Films. ACS Appl. Nano Mater. **1:** 1959–1967. doi:10.1021/acsanm.8b00452

Laspidou, C.S., Rittmann, B.E., (2002). A unified theory for extracellular polymeric substances, soluble microbial products, and active and inert biomass. Water Res. **36:** 2711–2720. doi:10.1016/S0043-1354(01)00413-4

Lau, P.S., Tam, N.F.Y., Wong, Y.S., (1998). Effect of carrageenan immobilization on the physiological activities of *Chlorella vulgaris*. Bioresour. Technol. **63:** 115–121. doi:10.1016/S0960-8524(97)00111-9

Lau, P.S., Tam, N.F.Y., Wong, Y.S., (1996). Wastewater nutrients removal by *Chlorella vulgaris*: Optimization through acclimation. Environ. Technol. (United Kingdom) **17:** 183–189. doi:10.1080/09593331708616375

Laurinavichene, T. V., Fedorov, A.S., Ghirardi, M.L., Seibert, M., Tsygankov, A.A., (2006). Demonstration of sustained hydrogen photoproduction by immobilized, sulfur-deprived *Chlamydomonas reinhardtii* cells. Int. J. Hydrogen Energy **31:** 659–667. doi:10.1016/j.ijhydene.2005.05.002

Lavrinovičs, A., Juhna, T., (2017). Review on Challenges and Limitations for Algae-Based Wastewater Treatment. Constr. Sci. **20:** 17–25. doi:10.2478/cons-2017-0003

Le Quéré, C., Andres, R.J., Boden, T., Conway, T., Houghton, R.A., House, J.I., Marland, G., Peters, G.P., van der Werf, G., Ahlström, A., Andrew, R.M., Bopp, L., Canadell, J.G., Ciais, P., Doney, S.C., Enright, C., Friedlingstein, P., Huntingford, C., Jain, A.K., Jourdain, C., Kato, E., Keeling, R.F., Klein Goldewijk, K., Levis, S., Levy, P., Lomas, M., Poulter, B., Raupach, M.R., Schwinger, J., Sitch, S., Stocker, B.D., Viovy, N., Zaehle, S., Zeng, N., (2012). The global carbon budget 1959–2011. Earth Syst. Sci. Data Discuss. **5:** 1107–1157. doi:10.5194/essdd-5-1107-2012

Lee, K.Y., Mooney, D.J., (2012). Alginate: Properties and biomedical applications. Prog. Polym. Sci. **37:** 106–126. doi:10.1016/j.progpolymsci.2011.06.003

Lee, R.A., Lavoie, J.-M., (2013). From first- to third-generation biofuels: Challenges of producing a commodity from a biomass of increasing complexity. Anim. Front. **3:** 6–11. doi:10.2527/a

Lee, R.E., (2008). Phycology, 4th ed. Cambridge University Press, Cambridge. doi:DOI: 10.1017/CBO9780511812897f.2013-0010

Leino, H., Kosourov, S.N., Saari, L., Sivonen, K., Tsygankov, A.A., Aro, E.M., Allahverdiyeva, Y., (2012). Extended H_2 photoproduction by N_2-fixing cyanobacteria immobilized in thin alginate films. Int. J. Hydrogen Energy **37:** 151–161. doi:10.1016/j.ijhydene.2011.09.088

Levalley, T.L., Richard, A.R., Fan, M., (2014). The progress in water gas shift and steam reforming hydrogen production technologies - A review. Int. J. Hydrogen Energy **39:** 16983–17000. doi:10.1016/j.ijhydene.2014.08.041

Li, H., Wang, S., Zhang, Y., Chen, L., (2018). High-level expression of a thermally stable alginate lyase using pichia pastoris, characterization and application in producing brown alginate oligosaccharide. Mar. Drugs **16:** doi:10.3390/md16050158

Lichtenthaler, H.K., (1987). Chlorophylls and Carotenoids: Pigments of Photosynthetic Biomembranes. Methods Enzymol. **148:** 350–382. doi:10.1016/0076-6879(87)48036-1

Little, B.J., Depalma, J.R., (2013). Marine biofouling. Mater. Mar. Syst. Struct. Treatise Mater. Sci. Technol. **28:** 89.

Liu, J., Cheng, F., Grénman, H., Spoljaric, S., Seppälä, J., Eriksson, J.E., Willför, S., Xu, C., (2016). Development of nanocellulose scaffolds with tunable structures to support 3D cell culture. Carbohydr. Polym. **148:** 259–271. doi:10.1016/j.carbpol.2016.04.064

Liu, Y., Sotelo-Boyás, R., Murata, K., Minowa, T., Sakanishi, K., (2011). Hydrotreatment of vegetable oils to produce bio-hydrogenated diesel and liquefied petroleum gas fuel over catalysts containing sulfided Ni-Mo and solid acids. Energy and Fuels **25:** 4675–4685. doi:10.1021/ef200889e

Liu, Z., Zhang, F., Chen, F., (2013). High throughput screening of CO_2-tolerating microalgae using GasPak bags. Aquat. Biosyst. **9:** 1–7. doi:10.1186/2046-9063-9-23

Lundquist, T.J., Woertz, I.C., Quinn, N.W.T., Benemann, J.R., (2010). A realistic technology and engineering assessment of algae biofuel production. Energy Biosciences Institute, Berkeley, California (2010)

Lynch, F., Santana-Sánchez, A., Jämsä, M., Sivonen, K., Aro, E.-M., Allahverdiyeva, Y., (2015). Screening native isolates of cyanobacteria and a green alga for integrated wastewater treatment, biomass accumulation and neutral lipid production. Algal Res. **11:** 411–420. doi:10.1016/j.algal.2015.05.015

Ma, J., Qin, B., Paerl, H.W., Brookes, J.D., Wu, P., Zhou, J., Deng, J., Guo, J., Li, Z., (2015). Green algal over cyanobacterial dominance promoted with nitrogen and phosphorus additions in a mesocosm study at Lake Taihu, China. Environ. Sci. Pollut. Res. **22:** 5041–5049. doi:10.1007/s11356-014-3930-4

Martin, S., Parton, R.G., (2006). Lipid droplets: a unified view of a dynamic organelle. Nat. Rev. Mol. Cell Biol. **7:** 373.

Masukawa, M. Mochimaru, H. Sakurai, H., (2002). Disruption of the uptake hydrogenase gene, but not of the bidirectional hydrogenase gene, leads to enhanced photobiological hydrogen production by the nitrogen-fixing cyanobacterium *Anabaena* sp. PCC 7120. Appl. Microbiol. Biotechnol. **58:** 618–624. doi:10.1007/s00253-002-0934-7

Matuszyńska, A., Ebenhöh, O., (2015) A reductionist approach to model photosynthetic self-regulation in eukaryotes in response to light. Biochem. Soc. Trans. **43:** 1133 LP-1139. doi:10.1042/BST20150136

Mautner, A., Lee, K.-Y., Lahtinen, P., Hakalahti, M., Tammelin, T., Li, K., Bismarck, A., (2014). Nanopapers for organic solvent nanofiltration. Chem. Commun. **50:** 5778–5781. doi:10.1039/C4CC00467A

McGlade, C., Ekins, P., (2015). The geographical distribution of fossil fuels unused when limiting global warming to 2°C. Nature **517:** 187–190. doi:10.1038/nature14016

Melero, J.A., Vicente, G., Morales, G., Paniagua, M., Bustamante, J., (2010). Oxygenated compounds derived from glycerol for biodiesel formulation: Influence on EN 14214 quality parameters. Fuel **89:** 2011–2018. doi:10.1016/j.fuel.2010.03.042

Melis, A., Happe, T., (2001). Hydrogen production. Green algae as a source of energy. Plant Physiol. **127:** 740–8. doi:10.1104/PP.010498

Monshupanee, T., Incharoensakdi, A., (2014). Enhanced accumulation of glycogen, lipids and polyhydroxybutyrate under optimal nutrients and light intensities in the cyanobacterium *Synechocystis* sp. PCC 6803. J. Appl. Microbiol. **116:** 830–838. doi:10.1111/jam.12409

Montemezzani, V., Duggan, I.C., Hogg, I.D., Craggs, R.J., (2015). A review of potential methods for zooplankton control in wastewater treatment High Rate Algal Ponds and algal production raceways. Algal Res. **11:** 211–226. doi:10.1016/j.algal.2015.06.024

Moreno-Garrido, I., (2008). Microalgae immobilization: Current techniques and uses. Bioresour. Technol. **99:** 3949–3964. doi:10.1016/j.biortech.2007.05.040

Morgan-kiss, R.M., Priscu, J.C., Pocock, T., Gudynaite-savitch, L., Huner, N.P.A., Morgan-kiss, R.M., Priscu, J.C., Pocock, T., Gudynaite-savitch, L., Huner, N.P.A., (2006). Adaptation and Acclimation of Photosynthetic Microorganisms to Permanently Cold Environments. Microbiol Mol Biol Rev. **70:** 222–252. doi:10.1128/MMBR.70.1.222

Mullineaux, C.W., (2014). Electron transport and light-harvesting switches in cyanobacteria. Front. Plant Sci. **5:** 7. doi:10.3389/fpls.2014.00007

Nagy, V., Podmaniczki, A., Vidal-Meireles, A., Tengölics, R., Kovács, L., Rákhely, G., Scoma, A., Tóth, S.Z., (2018). Water-splitting-based, sustainable and efficient H_2 production in green algae as achieved by substrate limitation of the Calvin–Benson–Bassham cycle. Biotechnol. Biofuels **11:** 69. doi:10.1186/s13068-018-1069-0

Naik, S.N., Goud, V. V., Rout, P.K., Dalai, A.K., (2010). Production of first and second generation biofuels: A comprehensive review. Renew. Sustain. Energy Rev. **14:** 578–597. doi:10.1016/j.rser.2009.10.003

Nair Aneesh, C., Haridas, A., Balakrishnan Manilal, V., (2015). Role of Nutrients Input Pattern on the Growth Dynamics of Common Freshwater Microalgal Community. Am. J. Plant Sci. **6:** 2481–2491. doi:10.4236/ajps.2015.615250

Narala, R.R., Garg, S., Sharma, K.K., Thomas-Hall, S.R., Deme, M., Li, Y., Schenk, P.M., (2016). Comparison of Microalgae Cultivation in Photobioreactor, Open Raceway Pond, and a Two-Stage Hybrid System. Front. Energy Res. **4:** 1–10. doi:10.3389/fenrg.2016.00029

Ohse, S., Derner, R.B., Ozório, R.Á., Corrêa, R.G., Furlong, E.B., Cesar, P., Cunha, R., (2015). Lipid content and fatty acid profiles in ten species of microalgae. Idesia (Arica) **33:** 93–102. Published by Universidad de Tarapacá. Facultad de Ciencias Agronómicas

Osundeko, O., Dean, A.P., Davies, H., Pittman, J.K., (2014). Acclimation of microalgae to wastewater environments involves increased oxidative stress tolerance activity. Plant Cell Physiol. **55:** 1848–1857. doi:10.1093/pcp/pcu113

Pandey, S., Rai, R., Rai, L.C., (2012). Proteomics combines morphological, physiological and biochemical attributes to unravel the survival strategy of *Anabaena* sp. PCC7120 under arsenic stress. J. Proteomics **75:** 921–937. doi:10.1016/j.jprot.2011.10.011

Park, J., Kim, D., Lee, J., Park, S., Kim, Y., Lee, J., (2008). Blending effects of biodiesels on oxidation stability and low temperature flow properties **99:** 1196–1203. doi:10.1016/j.biortech.2007.02.017

Parker, C.T., Tindall, B.J., Garrity, G.M., (2015). International Code of Nomenclature of Prokaryotes. Int. J. Syst. Evol. Microbiol. **69(1A):**S1-S111 doi:10.1099/ijsem.0.000778

Peltier, G., Thibault, P., (1985). O_2 Uptake in the Light in *Chlamydomonas*. Plant Physiol. **79:** 225–230.

Peramuna, A., Summers, M.L., (2014). Composition and occurrence of lipid droplets in the cyanobacterium *Nostoc punctiforme*. Arch. Microbiol. **196:** 881–890. doi:10.1007/s00203-014-1027-6

Peschek, G. a, Obinger, C., Paumann, M., (2004). The respiratory chain of blue-green algae (cyanobacteria). Physiol. Plant. **120:** 358–369. doi:10.1111/j.1399-3054.2004.00274.x

Pinzi, S., Garcia, I.L., Lopez-Gimenez, F.J., DeCastro, M.D.L., Dorado, G., Dorado, M.P., (2009). The ideal vegetable oil-based biodiesel composition: A review of social, economical and technical implications. Energy and Fuels **23:** 2325–2341. doi:10.1021/ef801098a

Pitt, F.D., Mazard, S., Humphreys, L., Scanlan, D.J., (2010). Functional characterization of *Synechocystis* sp. strain PCC 6803 pst1 and pst2 gene clusters reveals a novel strategy for phosphate uptake in a freshwater cyanobacterium. J. Bacteriol. **192:** 3512–3523. doi:10.1128/JB.00258-10

Pittman, J.K., Dean, A.P., Osundeko, O., (2011). The potential of sustainable algal biofuel production using wastewater resources. Bioresour. Technol. **102:** 17–25. doi:10.1016/j.biortech.2010.06.035

Porra, R.J., Thompson, W. a, Kriedemann, P.E., (1989). Determination of Accurate Extinction Coefficients and Simultaneous-Equations for Assaying Chlorophyll-a and Chlorophyll-B Extracted with 4 Different Solvents - Verification of the Concentration of Chlorophyll Standards by Atomic-Absorption Spectroscopy. Biochim. Biophys. Acta **975:** 384–394. doi:Doi 10.1016/S0005-2728(89)80347-0

Powell, N., Shilton, A., Chisti, Y., Pratt, S., (2009). Towards a luxury uptake process via microalgae - Defining the polyphosphate dynamics. Water Res. **43:** 4207–4213. doi:10.1016/j.watres.2009.06.011

Pratoomyot, J., Srivilas, P., Noiraksar, T., (2005). Fatty acids composition of 10 microalgal species. Songklanakarin J. Sci. Technol. **27:** 1179–1187.

Pröschold, T., Harris, E.H., Coleman, A.W., (2005). Portrait of a species: *Chlamydonomas reinhardtii*. Genetics **170:** 1601–1610. doi:10.1534/genetics.105.044503

Qi, F., Xu, Y., Yu, Y., Liang, X., Zhang, L., Zhao, H., Wang, H., (2017). Enhancing growth of *Chlamydomonas reinhardtii* and nutrient removal in diluted primary piggery wastewater by elevated CO_2 supply. Water Sci. Technol. **75:** 2281–2290. doi:10.2166/wst.2017.111

Rajan, K., Carrier, D.J., (2014). Characterization of rice straw prehydrolyzates and their effect on the hydrolysis of model substrates using a commercial endo -cellulase, β-glucosidase and cellulase cocktail. ACS Sustain. Chem. Eng. **2:** 2124–2130. doi:10.1021/sc5002947

Rajaniemi-Wacklin, P., Rantala, A., Mugnai, M.A., Turicchia, S., Ventura, S., Komárková, J., Lepistö, L., Sivonen, K., (2006). Correspondence between phylogeny and morphology of *Snowella* spp. and Woronichinia naegeliana, cyanobacteria commonly occurring in lakes. J. Phycol. **42:** 226–232. doi:10.1111/j.1529-8817.2006.00179.x

Ramachandran, R., Menon, R.K., (1998). An overview of industrial uses of hydrogen. Int. J. Hydrogen Energy **23:** 593–598. doi:10.1016/S0360-3199(97)00112-2

Ramos, M.J., Fernández, C.M., Casas, A., Rodríguez, L., Pérez, Á., (2009). Influence of fatty acid composition of raw materials on biodiesel properties. Bioresour. Technol. **100:** 261–268. doi:10.1016/j.biortech.2008.06.039

Redfield, A.C., (1934). On the proportions of organic derivatives in sea water and their relation to the composition of plankton. James Johnstone Meml. Vol. 176–192.

Rich, V.I., Maier, R.M., (2015). Chapter 6 - Aquatic Environments, in: Pepper, I.L., Gerba, C.P., Gentry, T.J.B.T.-E.M. (Third E. (Eds.), . Academic Press, San Diego, pp. 111–138. doi:https://doi.org/10.1016/B978-0-12-394626-3.00006-5

Ritchie, R.J., Trautman, D.A., Larkum, A.W.D., (1997). Phosphate Uptake in the Cyanobacterium *Synechococcus* R-2 PCC 7942. Plant Cell Physiol. **38:** 1232–1241. doi:10.1093/oxfordjournals.pcp.a029110

Romero, E., Novoderezhkin, V.I., Van Grondelle, R., (2017). Quantum design of photosynthesis for bio-inspired solar-energy conversion. Nature **543:** 355–365. doi:10.1038/nature22012

Rumeau, D., Peltier, G., Cournac, L., (2007). Chlororespiration and cyclic electron flow around PSI during photosynthesis and plant stress response. Plant, Cell Environ. **30:** 1041–1051. doi:10.1111/j.1365-3040.2007.01675.x

Ryckebosch, E., Muylaert, K., Foubert, I., (2012). Optimization of an analytical procedure for extraction of lipids from microalgae. J. Am. Oil Chem. Soc. **89:** 189–198. doi:10.1007/s11746-011-1903-z

Saad, O.A.L.O., Conrad, R., (1993). Temperature dependence of nitrification, denitrification, and turnover of nitric oxide in different soils. Biol. Fertil. Soils **15:** 21–27. doi:10.1007/BF00336283

Saito, T., Nishiyama, Y., Putaux, J.L., Vignon, M., Isogai, A., (2006). Homogeneous suspensions of individualized microfibrils from TEMPO-catalyzed oxidation of native cellulose. Biomacromolecules **7:** 1687–1691. doi:10.1021/bm060154s

Sakurai, H., Masukawa, H., Kitashima, M., Inoue, K., (2015). How close we are to achieving commercially viable large-scale photobiological hydrogen production by cyanobacteria: a review of the biological aspects. Life **5:** 997–1018. doi:10.3390/life5010997

Samori, G., Samori, C., Pistocchi, R., (2014). Nutrient removal efficiency and physiological responses of *Desmodesmus communis* at different HRTs and nutrient stress condition using different sources of urban wastewater effluents. Appl. Biochem. Biotechnol. **173:** 74–89. doi:10.1007/s12010-014-0792-7

Sanz-Luque, E., Chamizo-Ampudia, A., Llamas, A., Galvan, A., Fernandez, E., (2015). Understanding nitrate assimilation and its regulation in microalgae. Front. Plant Sci. **6:** 899 doi:10.3389/fpls.2015.00899

Schwenk, D., Seppälä, J., Spilling, K., Virkki, A., Tamminen, T., Oksman-Caldentey, K.M., Rischer, H., (2013). Lipid content in 19 brackish and marine microalgae: Influence of growth phase, salinity and temperature. Aquat. Ecol. **47:** 415–424. doi:10.1007/s10452-013-9454-z

Seibert, M., Torzillo, G., (2018). Microalgal Hydrogen Production, Comprehensive Series in Photochemical & Photobiological Sciences. The Royal Society of Chemistry. Croydon, UK, doi:http://dx.doi.org/10.1039/9781849737128

Sharma, B., Ahlert, R.C., (1977). Nitrification and nitrogen removal (in waste water treatment). Water Res **11:** 897–925.

Shi, J., Podola, B., Melkonian, M., (2007). Removal of nitrogen and phosphorus from wastewater using microalgae immobilized on twin layers: An experimental study. J. Appl. Phycol. **19:** 417–423. doi:10.1007/s10811-006-9148-1

Singh, B., 2013. Biofuel crop sustainability. John Wiley & Sons, Inc, Fort Valley, US, doi:10.1002/9781118635797

Singh, M., Das, K.C., (2014). Low Cost Nutrients for Algae Cultivation, in: Algal Biorefineries. Springer Netherlands, Dordrecht, pp. 69–82. doi:10.1007/978-94-007-7494-0_3

Singh, R.N., Sharma, S., (2012). Development of suitable photobioreactor for algae production - A review. Renew. Sustain. Energy Rev. **16:** 2347–2353. doi:10.1016/j.rser.2012.01.026

Singh, S.K., Sundaram, S., Kishor, K., (2014). Photosynthetic microorganisms: Mechanism for carbon concentration. 1st ed. Cham, Switzerland: Springer International Publishing.

Singh, S.P., Singh, P., (2014). Effect of CO_2 concentration on algal growth: A review. Renew. Sustain. Energy Rev. **38:** 172–179. doi:10.1016/j.rser.2014.05.043

Smith, D.R., (2017). Does Cell Size Impact Chloroplast Genome Size? Front. Plant Sci. **8:** 2116. doi:10.3389/fpls.2017.02116

Solovchenko, A., Khozin-Goldberg, I., (2013). High-CO_2 tolerance in microalgae: Possible mechanisms and implications for biotechnology and bioremediation. Biotechnol. Lett. **35:** 1745–1752. doi:10.1007/s10529-013-1274-7

Stanier, R.Y., Van Niel, C.B., (1962). The concept of a bacterium. Arch. Mikrobiol. **42:** 17–35.

Stanier, R. Y., Sistrom, W. R., Hansen, T. A., Whitton, B. A., Castenholz, R. W., Pfennig, N., et al. (1978). Proposal to Place the Nomenclature of the Cyanobacteria (Blue-Green Algae) Under the Rules of the International Code of Nomenclature of Bacteria. Int. J. Syst. Evol. Microbiol. **28:** 335–336. doi:10.1099/00207713-28-2-335

Stearns, P.N., (2012). The Industrial Revolution in World History. Avalon Publishing. New York, US, Routledge.

Sun, L., Fang, L., Zhang, Z., Chang, X., Penny, D., Zhong, B., (2016). Chloroplast Phylogenomic Inference of Green Algae Relationships. Sci. Rep. **6:** 20528. doi:10.1038/srep20528

Takenaka, H., Yamaguchi, Y., 2014. Commercial-scale culturing of cyanobacteria: an industrial experience. . In Sharma NK, Rai AK, Stal LJ. (editors) Cyanobacteria an Economic Perspective Chichester, UK: Wiley Blackwell. p. 293–301

Talebi, A.F., Tabatabaei, M., Chisti, Y., (2014). BiodieselAnalyzer© : a user-friendly software for predicting the properties of prospective biodiesel. Biofuel Res. J. **2:** 55–57.

Tamagnini, P., Leitão, E., Oliveira, P., Ferreira, D., Pinto, F., Harris, D.J., Heidorn, T., Lindblad, P., (2007). Cyanobacterial hydrogenases: Diversity, regulation and applications. FEMS Microbiol. Rev. **31:** 692–720. doi:10.1111/j.1574-6976.2007.00085.x

Tang, D., Han, W., Li, P., Miao, X., Zhong, J., (2011). CO_2 biofixation and fatty acid composition of *Scenedesmus obliquus* and *Chlorella pyrenoidosa* in response to different CO_2 levels. Bioresour. Technol. **102:** 3071–3076. doi:10.1016/j.biortech.2010.10.047

Thornber, J.P., (1975). Chlorophyll-Proteins: Light-Harvesting and Reaction Center Components of Plants. Annu. Rev. Plant Physiol. **26:** 127–158. doi:10.1146/annurev.pp.26.060175.001015

Tomar, V., Sidhu, G.K., Nogia, P., Mehrotra, R., Mehrotra, S., (2017). Regulatory components of carbon concentrating mechanisms in aquatic unicellular photosynthetic organisms. Plant Cell Rep. **36:** 1671–1688. doi:10.1007/s00299-017-2191-3

Ulrich, H., Mohrholz, V., Nagel, K., Nausch, M., Siegel, H., Wasmund, N., (2009). Estuarine , Coastal and Shelf Science Phosphorus input by upwelling in the eastern Gotland Basin (Baltic Sea) in summer and its effects on filamentous cyanobacteria. Estuar. Coast. Shelf Sci. **83:** 434–442. doi:10.1016/j.ecss.2009.04.031

Umena, Y., Kawakami, K., Shen, J.R., Kamiya, N., (2011). Crystal structure of oxygen-evolving photosystem II at a resolution of 1.9Å. Nature **473:** 55–60. doi:10.1038/nature09913

Unnithan, V. V., Unc, A., Smith, G.B., (2014). Mini-review: A priori considerations for bacteria-algae interactions in algal biofuel systems receiving municipal wastewaters. Algal Res. **4:** 35–40. doi:10.1016/j.algal.2013.11.009

Van Den Hende, S., Beelen, V., Bore, G., Boon, N., Vervaeren, H., (2014). Up-scaling aquaculture wastewater treatment by microalgal bacterial flocs: From lab reactors to an outdoor raceway pond. Bioresour. Technol. **159:** 342–354. doi:10.1016/j.biortech.2014.02.113

Van Eerden, F.J., Melo, M.N., Frederix, P.W.J.M., Periole, X., Marrink, S.J., (2017). Exchange pathways of plastoquinone and plastoquinol in the photosystem II complex. Nat. Commun. **8:** 1–8. doi:10.1038/ncomms15214

Van Wychen, S., Laurens, L.M.L., (2013). Determination of Total Lipids as Fatty Acid Methyl Esters (FAME) by in situ Transesterification. NREL. 275–300

Vasilieva, S.G., Lobakova, E.S., Lukyanov, A.A., Solovchenko, A.E., (2016). Immobilized microalgae in biotechnology. Moscow Univ. Biol. Sci. Bull. **71:** 170–176. doi:10.3103/S0096392516030135

Vermaas, W.F., (2001). Photosynthesis and Respiration in Cyanobacteria. Encycl. Life Sci. **1:** 1-7. doi:10.1038/npg.els.0001670

Walther, T.C., Farese, R. V., (2009). The life of lipid droplets. Biochim. Biophys. Acta - Mol. Cell Biol. Lipids **1791:** 459–466. doi:10.1016/j.bbalip.2008.10.009

Wang, H., Nche-Fambo, F.A., Yu, Z., Chen, F., (2018). Using microalgal communities for high CO_2-tolerant strain selection. Algal Res. **35:** 253–261. doi:10.1016/j.algal.2018.08.038

Whang, D.R., Apaydin, D.H., (2018). Artificial Photosynthesis: Learning from Nature. ChemPhotoChem **2:** 148–160. doi:10.1002/cptc.201700163

White, D., 1919. The unmined supply of petroleum in the United States. SAE Transactions, 220-228 doi:10.4271/190011

Wilde, H.P.J. De, Londo, H.M., (2009). Market analysis biofuels Implications for the armed forces in the Netherlands. (No. ECN-E--09-039). Energy research Centre of the Netherlands ECN.

Williams, J.G.K., (1988). Construction of specific mutations in photosystem II photosynthetic reaction center by genetic engineering methods in *Synechocystis* 6803. Methods Enzymol. **167:** 766–778. doi:10.1016/0076-6879(88)67088-1

Williams, P.J.L.B., Laurens, L.M.L., (2010). Microalgae as biodiesel & biomass feedstocks: Review & analysis of the biochemistry, energetics & economics. Energy Environ. Sci. **3:** 554–590. doi:10.1039/b924978h

Xin, C., Addy, M.M., Zhao, J., Cheng, Y., Cheng, S., Mu, D., Liu, Y., Ding, R., Chen, P., Ruan, R., (2016). Comprehensive techno-economic analysis of wastewater-based algal biofuel production: A case study. Bioresour. Technol. **211:** 584–593. doi:10.1016/j.biortech.2016.03.102

Xin, L., Hong-ying, H., Ke, G., Ying-xue, S., (2010). Effects of different nitrogen and phosphorus concentrations on the growth, nutrient uptake, and lipid accumulation of a freshwater microalga *Scenedesmus* sp. Bioresour. Technol. **101:** 5494–5500. doi:10.1016/j.biortech.2010.02.016

Xin, L., Hong-Ying, H., Yu-Ping, Z., (2011). Growth and lipid accumulation properties of a freshwater microalga *Scenedesmus* sp. under different cultivation temperature. Bioresour. Technol. **102:** 3098–3102.

Yamori, W., Shikanai, T., (2016). Physiological Functions of Cyclic Electron Transport Around Photosystem I in Sustaining Photosynthesis and Plant Growth. Annu. Rev. Plant Biol. **67:** 81–106. doi:10.1146/annurev-arplant-043015-112002

Zehr, J.P., Waterbury, J.B., Turner, P.J., Montoya, J.P., Omoregie, E., Steward, G.F., Hansen, A., Karl, D.M., (2001). Unicellular cyanobacteria fix N_2 in the subtropical North Pacific Ocean. Nature **412:**635

Annales Universitatis Turkuensis

UNIVERSITY OF TURKU

Grano Oy, Turku , Finland 2019

ISBN 978-951-29-7683-6 (PRINT)
ISBN 978-951-29-7684-3 (PDF)
ISSN 0082-7002 (Print)
ISSN 2343-3175 (Online)